IEEE Access
Multidisciplinary | Rapid Review | Open Access Journal

Received July 25, 2020, accepted July 31, 2020, date of publication August 12, 2020, date of current version August 24, 2020.

Digital Object Identifier 10.1109/ACCESS.2020.3016011

Design and Implementation of Improved Three Port Converter and B4-Inverter Fed Brushless Direct Current Motor Drive System for Industrial Applications

SATHISH KUMAR SHANMUGAM[1], SASIKALA RAMACHANDRAN[2], SENTHILKUMAR ARUMUGAM[3], SANJEEVI PANDIYAN[4], ANAND NAYYAR[5,7], (Senior Member, IEEE), AND EKLAS HOSSAIN[6], (Senior Member, IEEE),

[1]Department of EEE, M. Kumarasamy College of Engineering, Karur 639113, India
[2]Department of ECE, Kongu Engineering College, Perundurai 638060, India
[3]Department of EEE, Chettinad College of Engineering and Technology, Puliyur 639114, India
[4]Key Laboratory of Advanced Process Control for Light Industry, Ministry of Education, Jiangnan University, Wuxi 214122, China
[5]Graduate School, Duy Tan University, Da Nang 550000, Vietnam
[6]Oregon Renewable Energy Center (OREC), Department of Electrical Engineering and Renewable Energy, Oregon Tech, Klamath Falls, OR 97601, USA
[7]Faculty of Information Technology, Duy Tan University, Da Nang 550000, Vietnam

Corresponding authors: Anand Nayyar (anandnayyar@duytan.edu.vn) and Eklas Hossain (eklas.hossain@oit.edu)

ABSTRACT With the proliferation of renewables and energy storage, inverters and converters are being updated to outperform their antecedents in every possible aspect for numerous applications in fields and industries. The proposed research involves the design and implementation of improved three interface converter, and B4-Inverter fed brushless direct electric current motor drive for industrial uses. The proposed integrated Three Port Converter (ITPC) and B4-Inverter fed Brushless Direct Current Motor (BLDC) drive is proposed targeting low or medium applications. The ITPC has been operated in unidirectional and going in both directions for accomplishing a built-in dual electric potential and power rate of flow control. besides, efficiency and the losses of the proposed converter are analyzed using three different domains, i.e., battery charging, discharging, and photovoltaic (PV) effectively. The results are validated by performing simulations of the proposed systems in MATLAB/Simulink. The validation results reveal that the proposed converter works under all three domains and that the losses in the PV domain are reduced compared to the other converters. Also, the average efficiency achieved is 80.95%. These results authenticate the application of the proposed converter to numerous applications pertaining to renewable energy resources and energy systems.

INDEX TERMS ITPC, BLDC, simulation, battery domains, B4-inverter, energy storage systems, three port converter, PV systems, microcontroller, maximum power point tracking.

I. INTRODUCTION

The constant development in demand for global energy along with the soaring awareness of the society about environmental effects due to the extended usage of fossil fuels has resulted in renewable energy sources, such as photovoltaic (PV) technology, to be popularly explored. Even though PV energy has gained significant attraction over the past few years, the discontinuous nature of PV systems and the low conversion efficiency concerning PV modules are the huge obstructions for exploiting the PV source on a massive scale [1]. Hence, various studies have been carried out to minimize such disadvantages. For the purpose of extracting the maximum power of the PVarray, the conventional implementation of the maximum power point tracking (MPPT) in stand-alone systems is usually achieved by serially connecting a DC-DC converter between the PV array and the load and then having a bidirectional DC-DC converter in a

The associate editor coordinating the review of this manuscript and approving it for publication was N. Prabaharan.

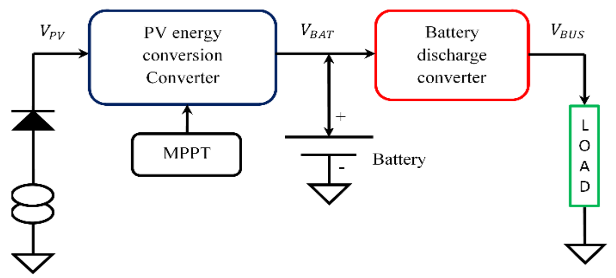

FIGURE 1. Block diagram of TPC with two-stage conversion, including the MPPT controller integrated with the PV energy and battery discharge converter.

parallel connection between the energy storage element and the load [2]. Energy storage element, such as the battery, is necessary for improving the system dynamics and steady-state characteristics. An Integrated Three Port Converter (ITPC) interfaced with solar, battery and motor, at the same time, can be considered to be a right candidate for a renewable power system and has gained a lot of research interest recently [3]–[5].

Conventionally, one PV energy converter is needed for the maximum power point tracking and then, the entire power is stored in a series-connected battery. Then one battery discharging converter is required for load voltage control in a standalone system, as illustrated in Figure 1—nonetheless, the system bulk and the cost of battery rise owing to this series setup. Meanwhile, the efficiency of the system reduces because of the two-stage conversion [6]. The two-stage converter requires complicated PWM controls as a more significant number of capacitors and diodes are required for controlling the output voltage and state (charge/discharge level) of the battery. As an alternative to reduce conversion stages, [7] one PV energy converter, one battery charging converter, and one battery discharging converter is proposed for standalone PV-battery system, as indicated in Figure 2. However, there is an increase in the system losses because of this sophisticated architecture. Modified multilevel cascaded H-bridge inverters have also been studied for use in PV systems [8].

Consecutively, to decrease the control losses, additional ITPC architecture is introduced in [9]–[15]. ITPC features include one stage conversion connecting two of the three ports, greater system efficiency, and a smaller quantity of components, quicker response, and integrated power management among the ports with central control. The ITPC design is illustrated in Figure 3. The current study explains the ITPC used B4-inverter fed BLDC motor drive system, as shown in Figure 4, having all the aforementioned benefits. In addition, it is possible to increase the total efficiency of the system in comparison with the existing one.

The choice of BLDC motors for this article emerged from their relative advantages over induction motors [16]. The B4-inverter is an alternative topology of the conventional B6 inverter, having six switches and six diodes [17].

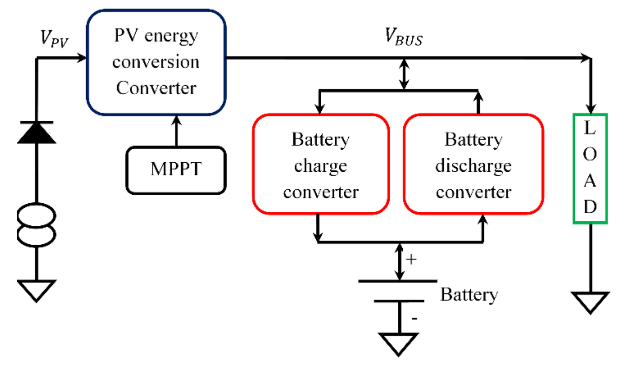

FIGURE 2. Block diagram of ITPC with single-stage conversion, taking battery charge and discharge converter into consideration for standalone PV battery system.

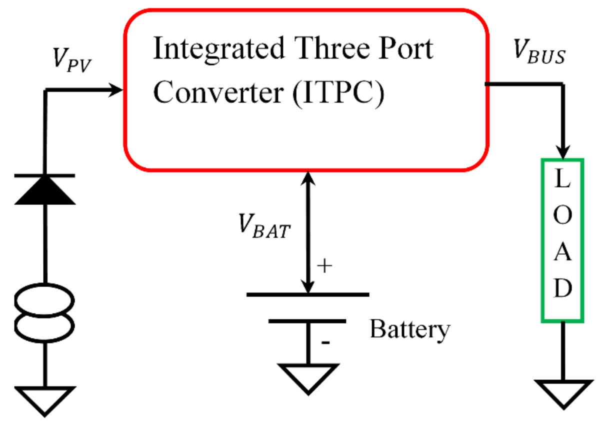

FIGURE 3. Block diagram of ITPC with single-stage conversion, connecting two of the three ports, a smaller quantity of components, and integrated power management among the ports with central control.

B4-inverter fed BLDC motor drives have garnered a lot of attention in several works. Researchers have worked on renewable energy fed BLDC drive with a DC-DC converter for reducing vibration and noise [18]. Several control schemes are prevalent for BLDC motor drives, such as FPGA based scheme [19]–[20], sensor-less control [21], [22], etc. Compared with the traditional inverter, the Z-source inverter has an extra shoot through switching state. During the shoot-through state, the output voltage to the load terminals is zero, i.e., both the thyristors of the same leg conduct simultaneously. This period helps in boosting the voltage of the Z-impedance network. This shoot-through period is forbidden in conventional inverters which destroy the inverter. This shoot-through period is controlled by varying the modulation index of the inverter and they are generated by various control methods proposed [23] [24].

In comparison to such works, the contributions of this technical work presented in the paper are:

1) The newly introduced ITPC converter is developed for boosting the overall efficiency of the standalone system.

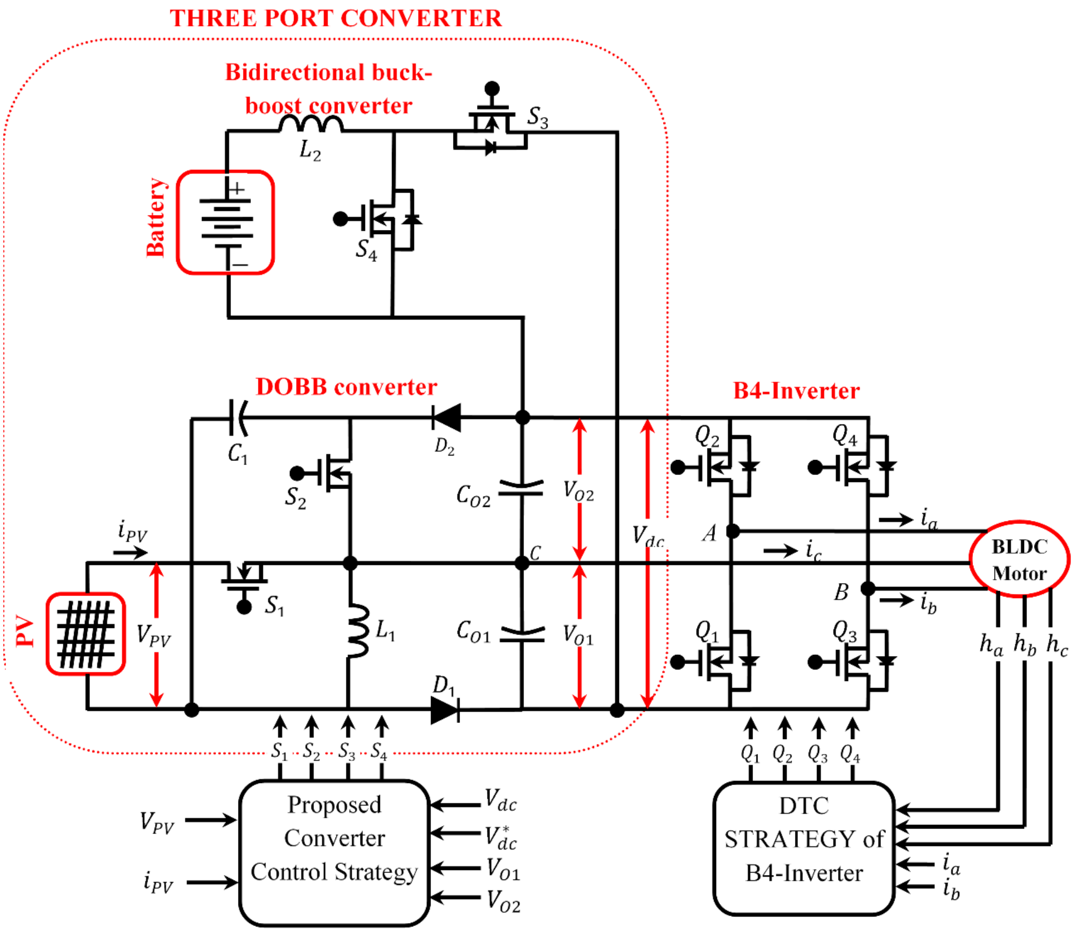

FIGURE 4. Conventional TPC employed B4-inverter fed BLDC motor drive system, providing an enhanced efficiency compared to the aforementioned ITPC, utilizing battery controlled converter circuit coupling at DC connection.

2) Because of the single-arrange control change, the current flow in the semiconductor device in the ITPC is greatly reduced.

3) The work also includes center tap voltage fluctuation control and DTC for torque ripple minimization while sector to sector commutations.

However, the ITPC has some drawbacks as stated below:

1. Structure needs galvanic isolation to ensure safety measures.

2. Maintenance is high.

3. Battery power is high.

4. Isolation of converter is high

Control Strategy of DOBB Converter:

The control mechanism is designed in order to achieve a stable voltage and control the current storage capacity of the topology in order to improve the dynamic response of the converter during the application of the load or input voltage disturbances. In the situation of the rise in input voltage or drop in load current that may result in over-voltage in the output, closed-loop regulation that senses the actual output voltage of the system and then activates the power switches in order to deviate the inductor current from the load and to eliminate the over-voltage is required. The case of drop-in input voltage or rise in load current is also solved by using closed-loop control strategies. The contribution done by the present research depends upon the SIMO DOBB converter by selecting a classical Proportional Integral (PI) controller for a closed-loop control strategy. The PI controller attempts to precise the error among the measured process variables and the desired set point through calculation and then provides an accurate output, consequently, it can control the conversion process. The PI controller computation involves two unique modes: proportional mode and integral mode. In the proportional mode, the reaction to the current error is decided, but in the integral mode, the reaction based recent error is decided. The weighted sum of the two modes provides the output to be the corrective action to the control element. PI controller is widely applied in several industries due to its simple design and unsophisticated structure.

$$output\ (t) = K_P err\ (t) + K_I \int_0^t err\ (t)\ dt \qquad (1)$$

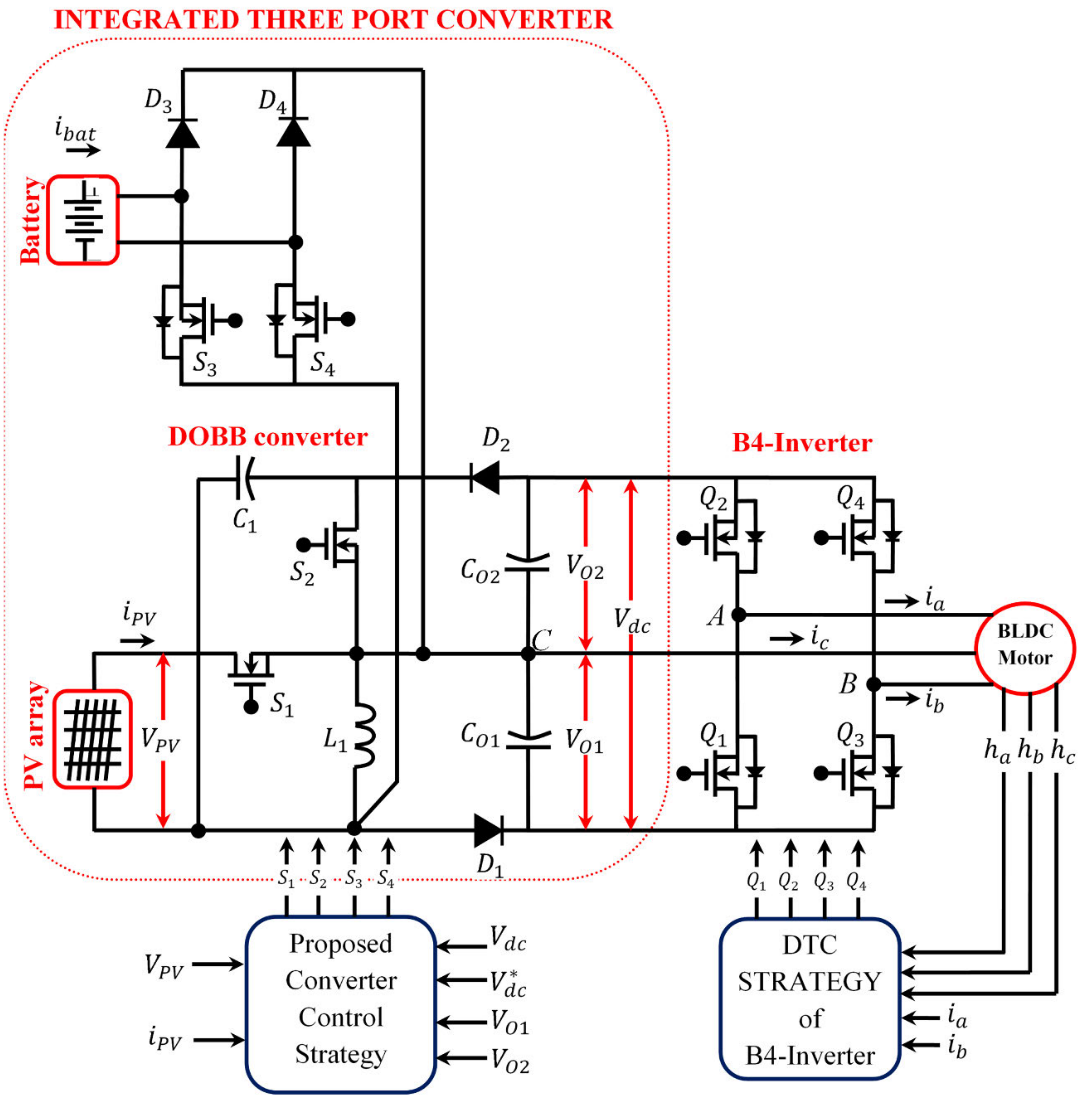

FIGURE 5. A substitute proposition of the ITPC converter for the execution of the B4-inverter fed BLDC motor drive system with a phase change framework.

where, $err(t) = set\ voltage - actualvoltage\ K_P, K_I$ are the proportional and integral controller gains respectively.

The rest of the paper is organized as follows: Section II sheds light on the materials and methods utilized in this article, including the architecture and working principle of the proposed system, the power flow analysis of the ITPC and its mathematical modeling, and the estimation of power losses in the ITPC converter. Section III contains the simulation results and discussions that include a comparative analysis of the proposed system with the conventional system in terms of losses and efficiency. Section IV describes the experimental analysis of the ITPC converter and the B4 inverter fed BLDC motor driver, encompassing the controller features, measurement devices, and circuits, gate driver circuits, hardware component selection along with the experimental results of the proposed ITPC. Finally, Section V concludes the paper with important findings.

II. MATERIALS AND METHODS

A. ARCHITECTURE AND WORKING PRINCIPLE OF PROPOSED SYSTEM

The ITPC with motor driver by one stage conversion system is illustrated in Figure 5. The proposed research consists of a solar array powered dual output buck-boost (DOBB) converter, B4-Inverter fed BLDC motor and ampere-hour powered battery, which acts as back-up power for the load operating under demand condition. The proposed DOBB converter comprises of buck-boost switch S_1, power-sharing switch S_2, two power diodes D_1 and D_2, a single buck-boost inductor L_1, intermediate capacitor C_1, and output capacitors C_{01} and C_{02}. Similarly, the bidirectional buck-boost converter consists of buck switch S_3, boost switch S_4 and power diodes D_3 and D_4. On the other side, the rear end B4-inverter comprises four switches Q_1 to Q_4 and a BLDC motor.

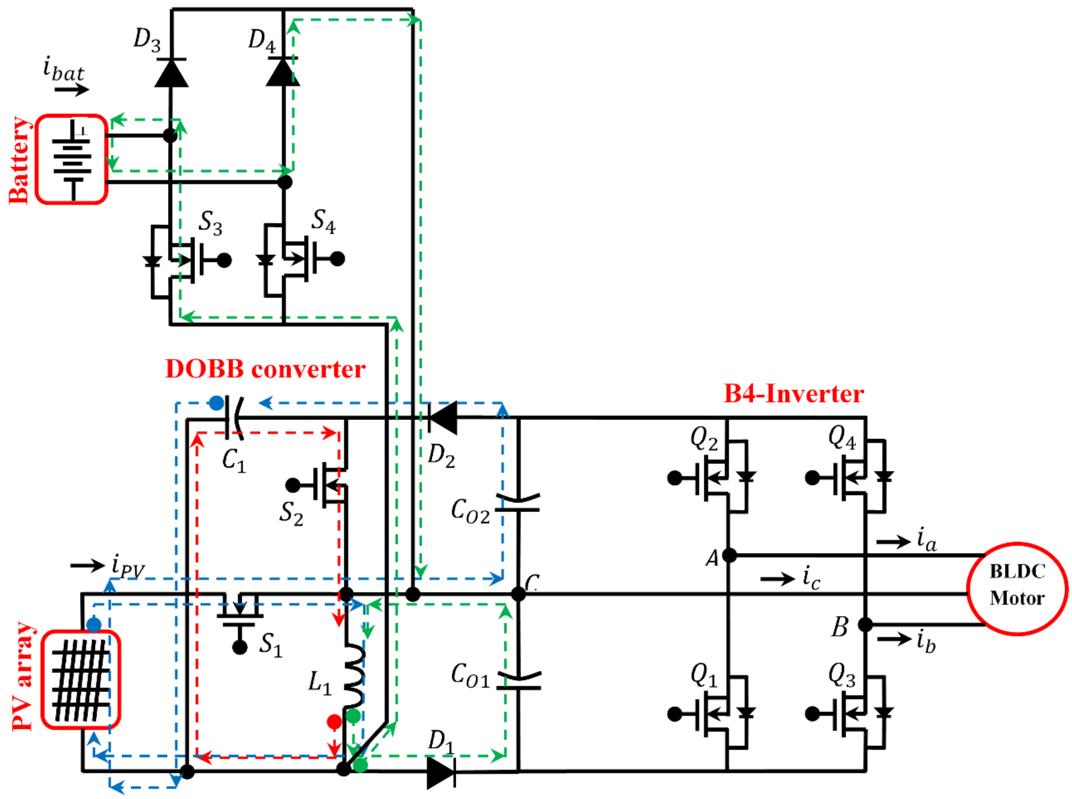

FIGURE 6. Equivalent circuit of ITPC operates in BCD, showing three different modes of operation in blue, green, and red dotted lines.

Figure 5 shows a substitute proposition of the converter (ITPC converter) for the execution of BLDC drive with a phase change framework. The battery-controlled converter circuit coupling at DC connection is utilized as shown in Figure4, which is particularly coupled at the inductor (L_1) terminal. The main advantage of this shape is that the DC-DC converter handles only a part of the power created, allowing for more noteworthy proficiency in correlation with DC between gathering correspondence coupling setup. An incorporated power circuit is exhibited in this specialized work alongside the underneath separate various limits, i.e., battery, battery buck controller, and step up/step down change and burden voltage guideline. The switch (S_1) present in the DOBB converter is for the extraction of the greatest power from the PV board utilizing the Perturb and Observe

(P&O) MPPT calculation. On the opposite side, the guideline of the all-out output voltage to the required worth is the obligation of the power-sharing switch (S_2) present in the DOBB converter. Likewise, when the produced voltage is adequate to drive the BLDC motor, the extra voltage is stored by the battery. When the power switch (S_3) is turned on, the inductor (L_1) stores the energy and energy flows from the PV module to the battery. If the voltage that is created at the PV module is insufficient to drive the BLDC motor, the power framework works as a lift converter, making the charges move from the battery to the BLDC motor. When the switch (S_4) is turned on, the inductor (L_1) stores the energy from the battery, and if the switch (S_4) is off, the energy stored in the inductor gets moved to the BLDC motor. The switches (S_3 and S_4) are correspondingly used.

B. POWER FLOW ANALYSIS OF ITPC

To demonstrate the dynamic output qualities of the PV module under various daylight conditions, the framework proposed will work in different power stream modes such as battery charging area (BCD), PV space (PVD) and battery releasing space (BDD).

In the Battery Charging Domain (BCD) mode, the PV charges the battery. The bidirectional converter works as a buck converter in the BCD. This happens if the PV power is extremely contrasted with the heap control and if the PV voltage is higher than the battery voltage required, indicating that the battery must be charged. In BCD, switches S_1, S_2, S_3 are dynamic and switch S_4 is in off condition. BCD has four modes, which are named as mode A, B, C, and D. In mode A, the switch, S_2, is turned on and switches S_1, S_3, S_4 are off. As S_2 is on, energy stored in the inductor L_1 moves to the capacitor C_1, and the capacitor begins to charge. The identical circuit of ITPC working in this mode is demonstrated as the red line in Figure 6. In mode B, the switch S_1 is turned on and switches S_2, S_3, S_4 are off. Since S_1 is on, the inductor

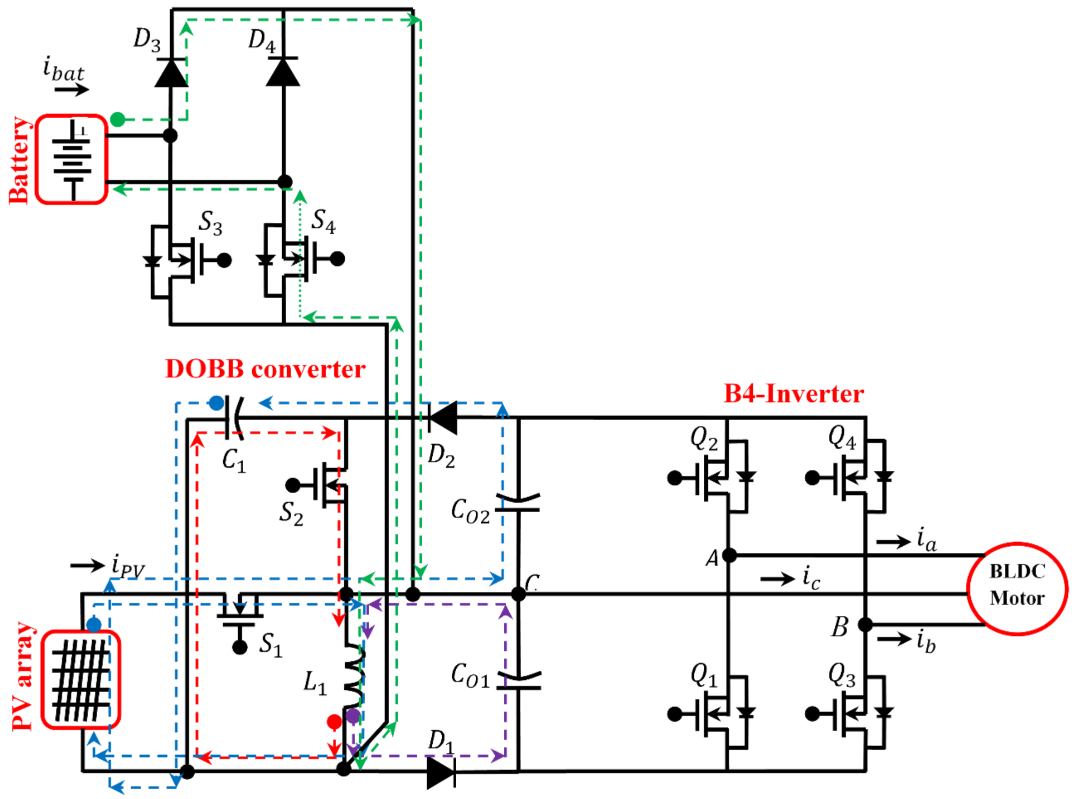

FIGURE 7. Equivalent circuit of the proposed converter operates in BDD, showing four different modes of operation as marked in blue, green, red and purple.

L_1 begins to charge from PV, and afterward, the current, i_{L1} increases. Then again, the current in the capacitor, i_{C1} and PV begin to release to the output capacitor, C_{O2} through the diode, D_2, and current, i_{C1} reduces, while the output capacitor current, I_{O2} increases. The proportional circuit of ITPC working in this mode demonstrated as the blue line in Figure 6. In mode C, the switch, S_3 is turned on and switches S_1, S_2, S_4 are turned off. Also, the extra energy in the inductor, L_1, moves to the battery, while the battery starts to charge. All the while, the

diode, D_1 is forward biased for making a flowing current way of the inductor, L_1, subsequently the capacitor, C_{O1} current increases. The identical circuit of ITPC working in this mode is demonstrated as a green line in Figure 6. In mode D, switches, S_2 and S_3 are turned on and switches S_1, S_4 are turned off. The extra energy present in the inductor, L_1 gets moved to the battery while the battery starts to charge. Simultaneously, the inductor, L_1, begins to release energy to the capacitor, C_1 through a switch, S_2, and the capacitor current, i_{C1} increases. The comparable circuit of ITPC working in this mode is signified as a green and red line in Figure 6 correspondingly.

In the PVD mode, the value of the load current is equal to the PV module current; the power that is handled by the bidirectional converter is zero. Here, the efficiency of the power network is near 95% since the most extreme intensity of the PV module gets moved to the load just by the DOBB converter. In PVD, switches S_1 and S_2 are dynamic and switches S_3 and S_4 are completely off.

In the BDD mode, both the sources PV and battery provide energy to the load. The bidirectional converter works as a boost converter either in the battery de-energize mode or if the load power demand is higher than the produced power. In BDD, switch, S_3 is turned off entirely, and switch S_1, S_2, S_4 are dynamic. The five various activity modes in BDD are modes H, I, J, K and L. In mode H, the switch, S_2 is turned on and switches S_1, S_3, S_4 are turned off. Since S_2 is on, the energy stored in the inductor L_1 flows to the capacitor C_1, and the capacitor begins to charge. The proportional circuit of ITPC working in this mode is shown as a red line in Figure 7. In mode I, the switch S_1 is turned on and switches S_2, S_3, S_4 are turned off. As S_1 is on, the inductor, L_1 begins to charge from PV, and the current, i_{L1} increases. Then again, the current in the capacitor C_1 and PV begins to release to output capacitor, C_{O2} through the diode D_2, while the output capacitor current increases. The equal circuit of ITPC working in this mode is meant as the blue line in Figure 7. In mode J, the switches S_1 and S_4 are turned on and switches S_2 and S_3 are turned off. In this way, the inductor, L_1 begins to charge from PV, while the current in the capacitor, C_1 and PV begin to release to output capacitor, C_{O2} through the diode, D_2. At the same time, the surplus load current gets removed from the battery and afterward put away in an inductor, L_1 through a switch, S_4 and diode, D_3. The comparable circuit of ITPC working in this mode is demonstrated as a green line in Figure 7. In mode K, switch S_4 is turned on and switches S_1, S_2 and S_3 are turned off. In this way, the surplus load current is removed from the battery and afterward, put away in an inductor, L_1, consequently, the inductor current increases. The identical circuit of ITPC working in this mode is shown as a green line in Figure 7. In mode, L switches S_1, S_2, S_3, and S_4 are turned off. In this way, the surplus current put away in an inductor, L_1 gets moved to the output capacitor, C_{O1}. The proportional circuit of ITPC working in this mode is signified as the purple line in Figure 7.

C. MATHEMATICAL MODELLING OF THE PROPOSED ITPC

The converter conduction at different time intervals and its modeling are shown in Figure 8. During the conduction at time interval 1 as represented in Figure 8(a), the governing equations are

$$L_1 \frac{di_{L1}}{dt} = -V_{C1} \quad (2)$$

$$C_{01} \frac{dV_{01}}{dt} = -\frac{V_{01}}{R_1} \quad (3)$$

$$C_{02} \frac{dV_{02}}{dt} = -\frac{V_{02}}{R_2} \quad (4)$$

During the conduction at time interval 2 as represented in Figure 8(b), the governing equations are

$$L_1 \frac{di_{L1}}{dt} = V_{in} \quad (5)$$

$$C_{01} \frac{dV_{01}}{dt} = -\frac{V_{01}}{R_1} \quad (6)$$

$$C_{02} \frac{dV_{02}}{dt} = \frac{V_{C1} + V_{in} - V_{02}}{R_2} \quad (7)$$

During the conduction at time interval 3 as represented in Figure 8(c), the governing equations are

$$L_1 \frac{di_{L1}}{dt} = -V_{01} \quad (8)$$

$$C_{01} \frac{dV_{01}}{dt} = i_{L1} - \frac{V_{01}}{R_1} \quad (9)$$

$$C_{02} \frac{dV_{02}}{dt} = -\frac{V_{02}}{R_2} \quad (10)$$

D. ESTIMATION OF POWER LOSSES IN ITPC CONVERTER

Conduction loss of the switch S_1 is

$$P_{cond-S1} = I_{S1}^2 \times R_{DS-on} \quad (11)$$

where, I_{S1} denotes the current flowing through the switch S_1, and R_{DS-on} represents the drain to source resistance of the switch when it is in a conducting state or on the state.

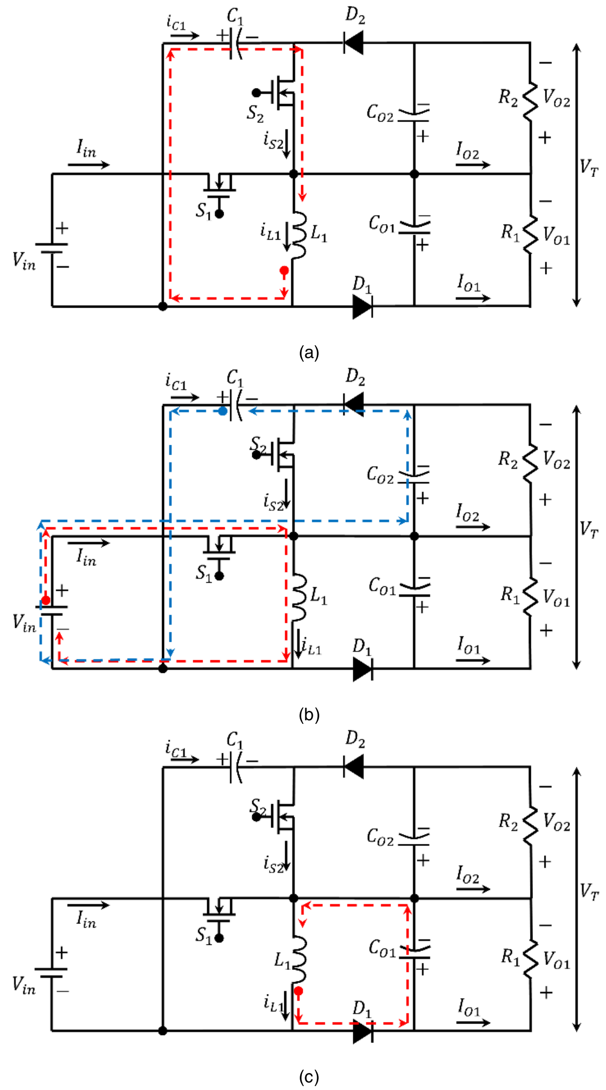

FIGURE 8. ITPC Conducting states at a time interval (a) 1; (b) 2; (c) 3, showing the flow of current in different modes of operation marked in red and blue.

III. SIMULATION RESULTS AND DISCUSSIONS

In order to verify the performance of the proposed system, at first, simulations have been done in ideal, battery discharging and charging modes by MATLAB software. Input voltage sources such as PV and battery are considered to be $V_{PV} = 18V$ and $V_{bat} = 12V$. The output voltages of the ITPC are desired to be regulated on $V_{O1} = 24$ V and $V_{O2} = 24$ V. Consequently, the total output voltage is desired to be regulated on 48 V. The simulation parameters of the proposed system are listed in Table 1. The following parameters such as PV insolation (IRR), PV Power (P_{PV}),

ITPC power (P_{dc}), BLDC motor rotor speed (N), Battery Power (P_{bat}), and state of charge ($SOC\%$) of the system are measured for validating the proposed idea.

The qualities of a 70 W PV module can be reproduced utilizing MATLAB instrument depending on the identical circuit model. Presently, the reproduction is analyzed in

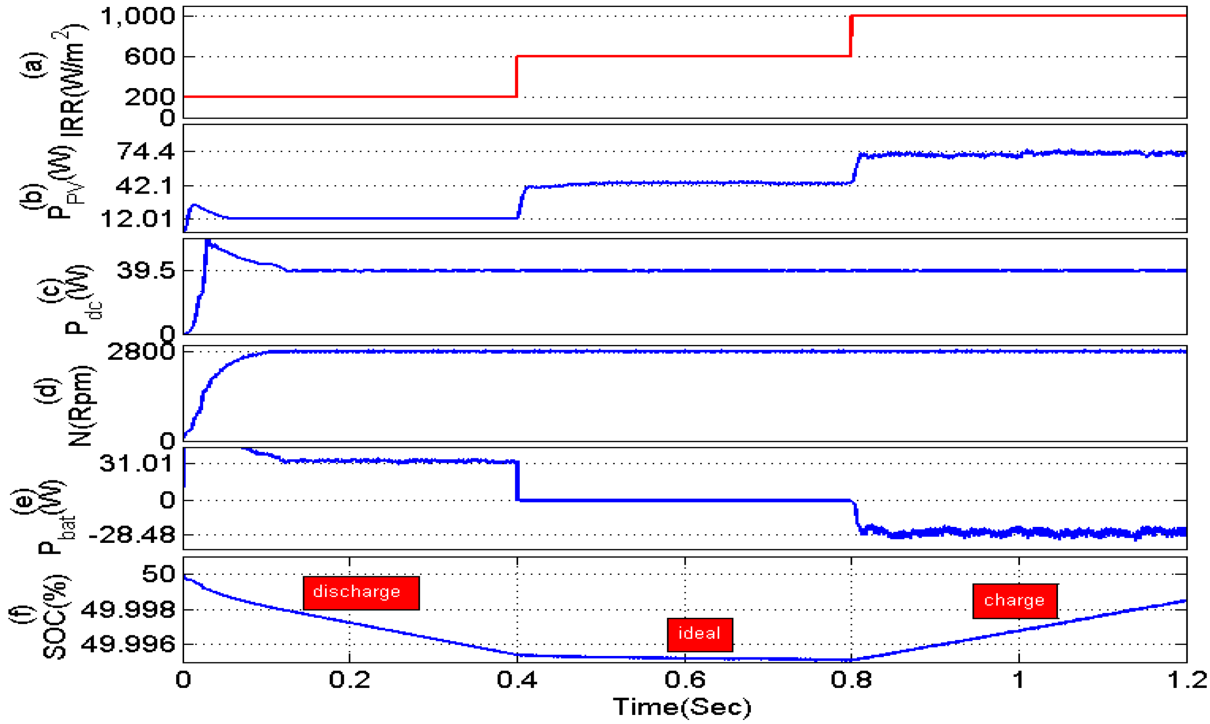

FIGURE 9. Performance validation of proposed system under different insolation condition showing (a) the most extreme insolation on PV, (b) the fluctuation of power, (c) the mechanical capacity to a load, (d) rotor speed, (e) voltage levels of battery connection, (f) SOC of the battery.

TABLE 1. Simulation specifications of the proposed system.

Sl. no.	Objects	Values
1	Maximum PV module voltage	18 V
2	Maximum PV module current	4.17 A
3	Maximum PV module power	75 W
4	ITPC output voltage	48 V
5	ITPC output power	40 W
6	Rated BLDC motor power (Torque = 0.125 Nm, Speed = 2800 Rpm, DC link voltage = 24V, number of poles = 8)	39 W
7	Nominal power of battery (Nominal voltage = 12 V, Nominal current = 7A/h)	84 W/h

three distinctive activity modes (for example, perfect, battery charging, and battery discharging) of ITPC. The simulation results for these three modes are depicted in detail. Initially (e.g., 0 to 0.4 Sec), the solar insolation of (200 W/m^2) is connected to the PV. At 0.4sec, the solar insolation is expanded all of a sudden from (200 to 600 W/m^2). At 0.8 sec, the most extreme insolation (i.e.1000 W/m^2) is connected on PV as appears in Figure 9(a). Because of changes in solar insolation, the power produced from PV fluctuates from (12.01 W, 42.1 W, and 74.4 W) separately, as can be seen in Figure 9(b). The BLDC motor of intensity rating 39W (rotor speed = 3000 rpm, evaluated DC-interface voltage = 24V, load torque = 0.125 Nm and the number of posts = 8) is taken at the load port of the proposed framework. The motor conveys 39.5 W of mechanical capacity to a load at 2800 rpm, as shown in Figure 9(c). Additionally, the rotor speed is kept up at 2800 rpm as shown in Figure 9(d) individually. At low insolation condition (i.e. 200 W/m^2), the required load power of 31.01W is effectively removed from the battery. At a specific moment, 11.8 V and +2.62 Amp are drawn from the battery. Likewise, at greatest insolation condition (i.e., 1000 W/m^2), the surplus PV intensity of 28.48 W is proficiently conveyed to the battery. At a specific moment, 12.3 V and - 2.32 Amp is connected towards the battery individually, appeared in Figure 9(e). Furthermore, at medium insolation condition (i.e., 600 W/m^2), the PV exclusively meets the load necessity. Therefore the battery is in perfect condition. As observed from Figure 9(e), the negative sign means that the battery acquires power from the PV; therefore, the positive sign shows that the battery gives power to the load. The state of charge (SOC) of the battery, at all the three modes, is depicted in Figure 9(f).

As observed in figure 9, the proposed research is constrained by planned compensators efficiently. Additionally, the power balance among data sources and outputs must be satisfied. The ITPC Converter ripple voltages are shown in Figure 10. ITPC offers versatility due to its capabilities in improving the output voltage control during the dynamic (sudden variation) in input voltage and load disturbances conditions. Moreover, for applications regarding the load or input voltage disturbance, DOBB converter control possesses the capability to eliminate the impact of these disturbances from the output voltages.

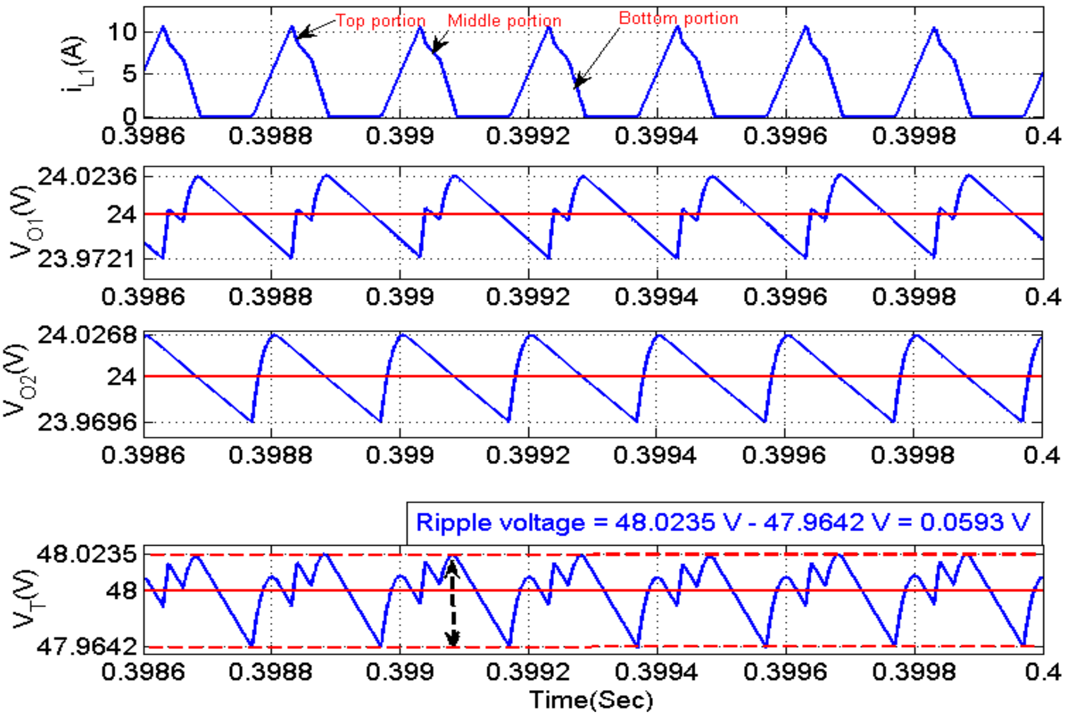

FIGURE 10. ITPC Converter ripple current i_{L1} and voltage V_{O1}, V_{O2} and V_T with respect to time.

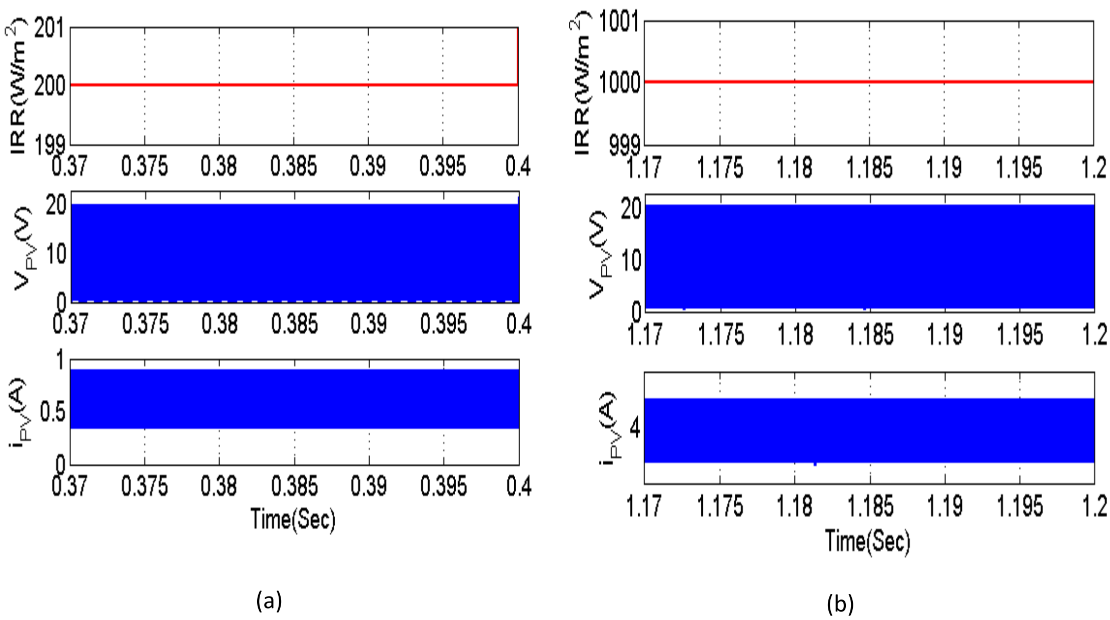

FIGURE 11. Solar unit at different irradiation (a) 200 W/m^2*and* (b) 1000 W/m^2.

The ITPC Converter Solar unit at different irradation (a) $200W/m^2 and$ (b) 1000 W/m^2 are shown in Figure11. The ITPC output voltage at different irradation, BLDC motor at different irradiation (a) 200 $W/m^2 and$ (b) 1000 W/m^2 are shown in Figures 12 & 13.

The charging units at different irradation (a) 200 $W/m^2 and$ (b) 1000 W/m^2 and BLDC motor parameters are shown in Figures 14& 15, respectively. A voltage follower approach is adjustable for controlling the Proposed converter when it operates with DCM. A dual voltage sensor, i.e., total output voltage and capacitor (C_{O2}) voltage measurement sensors, is necessary for regulating the output voltage of the DOBB converter. Figure 3.8 presents a closed-loop control of the DOBB converter. This control strategy comprises a voltage

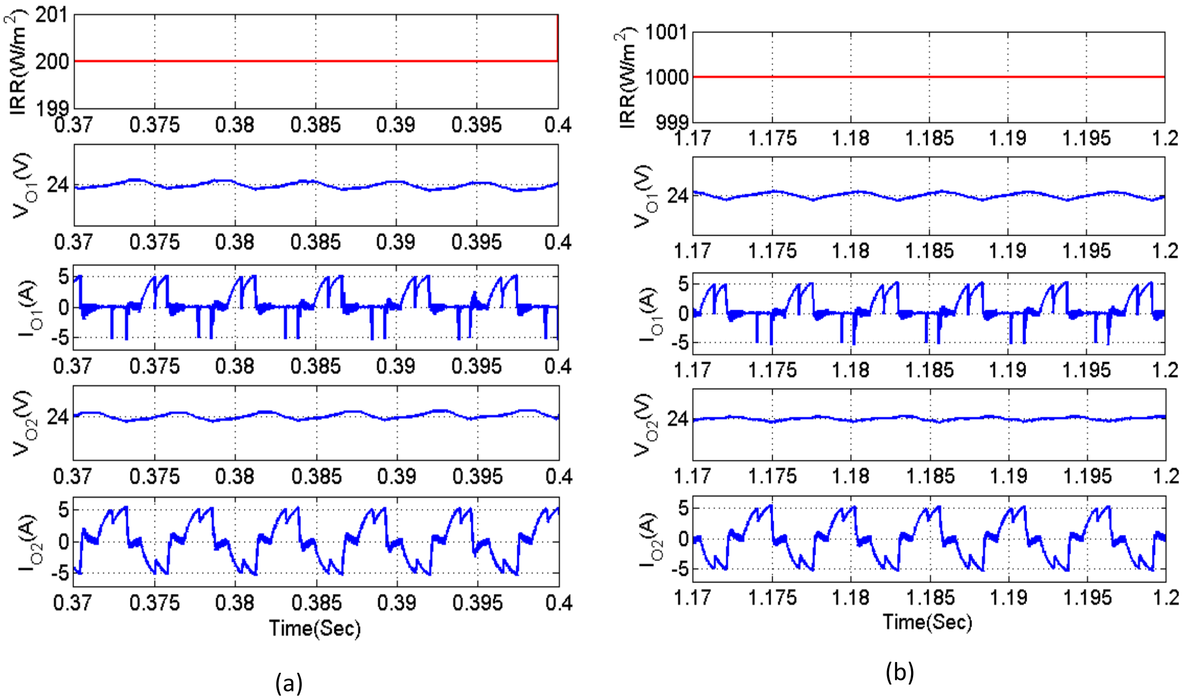

FIGURE 12. ITPC output voltage at different irradiation (a) 200 W/m^2 *and* (b) 1000 W/m^2.

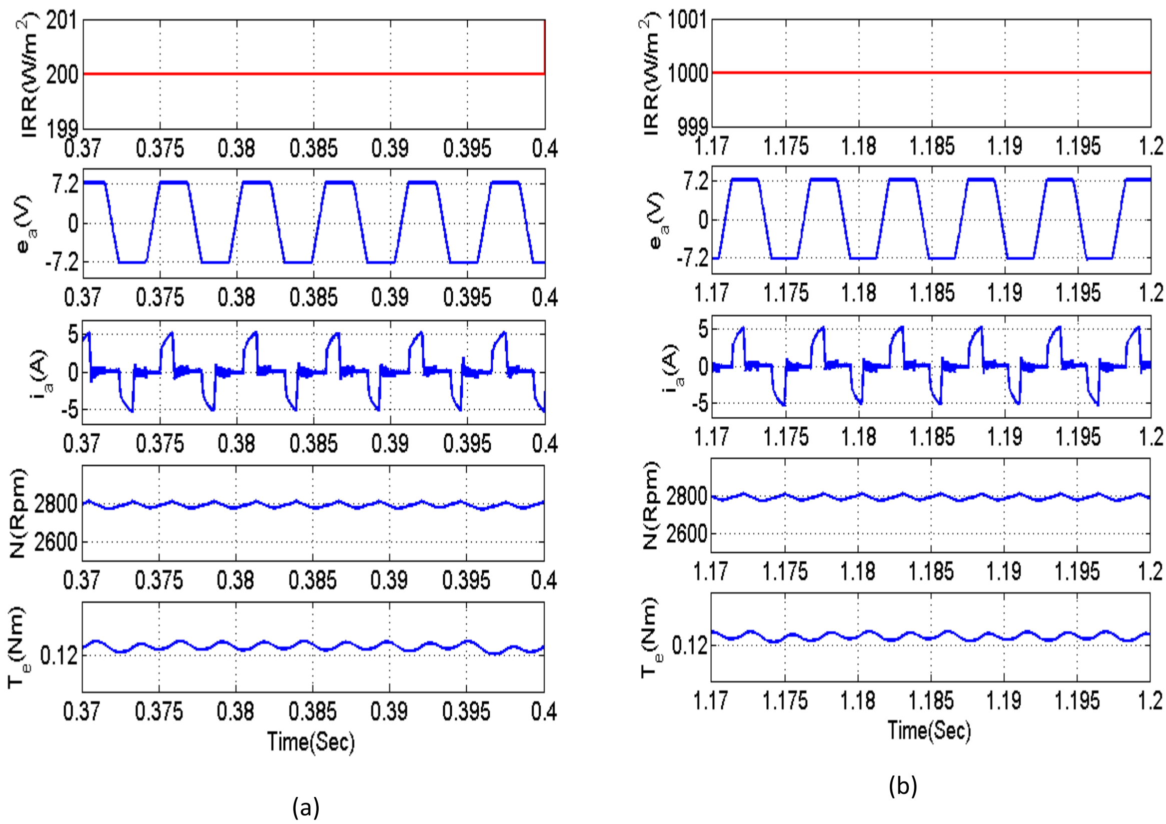

FIGURE 13. BLDC motor at different irradation (a) 200 W/m^2 *and* (b) 1000 W/m^2 (a) 200 W/m^2 (b) 1000 W/m^2.

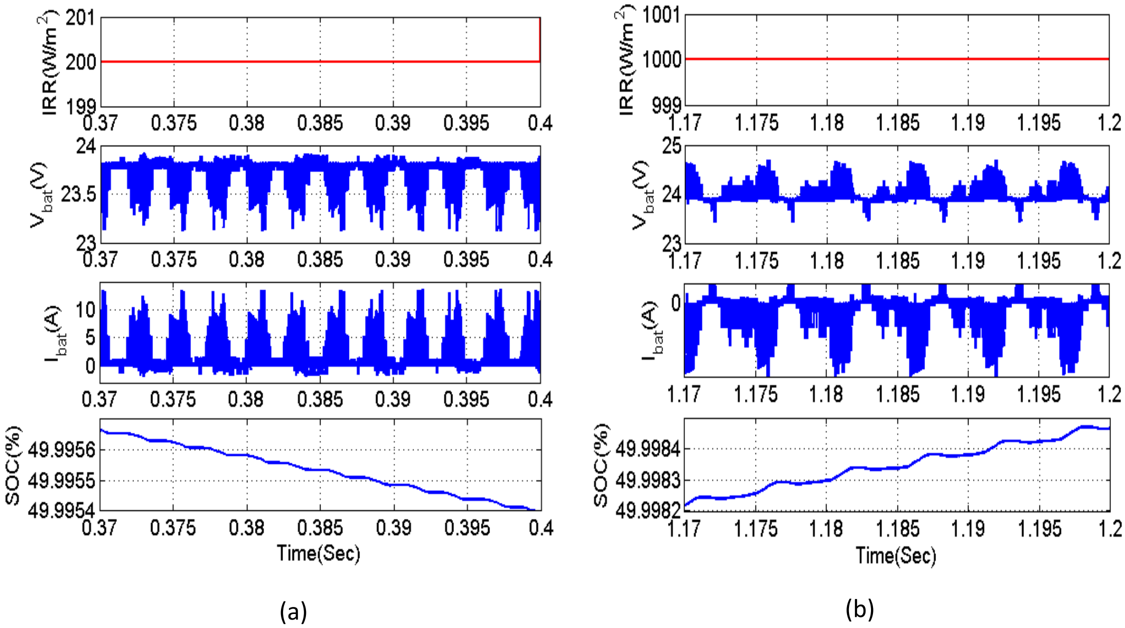

FIGURE 14. Charging unit at different irradiation (a) 200 W/m^2 and (b) 1000 W/m^2.

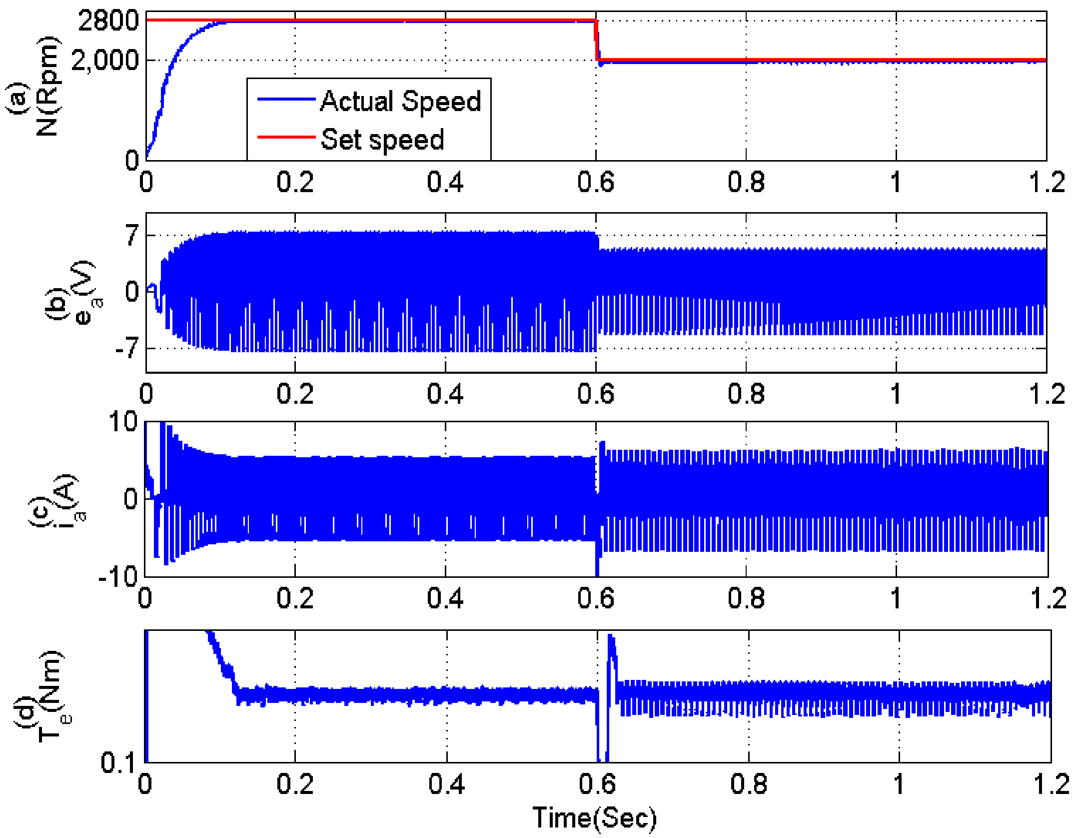

FIGURE 15. BLDC motor parameters and corresponding waveforms (a) actual and set speed in RPM, (b) Voltage (e_a), (c) Current (i_a), (d) Torque (T_e) with respect to time in seconds.

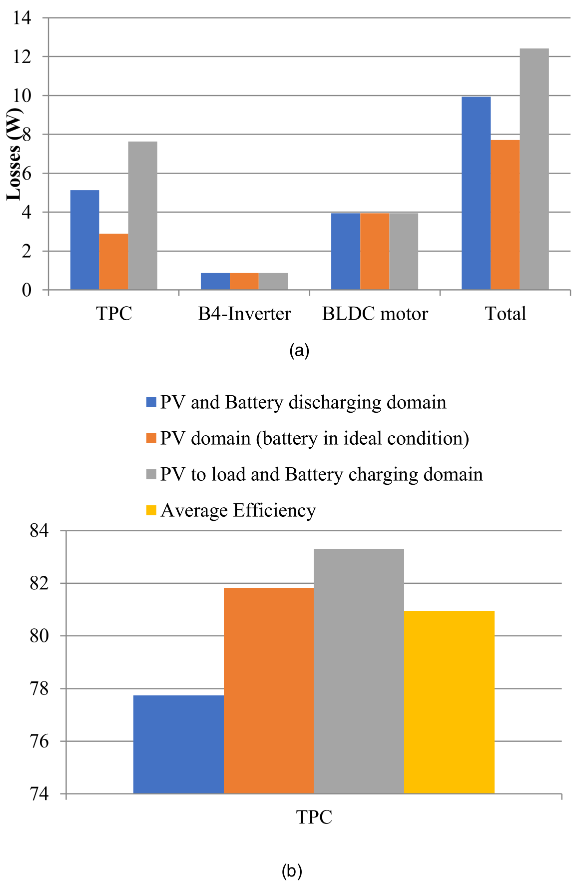

FIGURE 16. **Analysis in the proposed system under three different domains at two-stage conversions (a) Losses (b) Efficiency.**

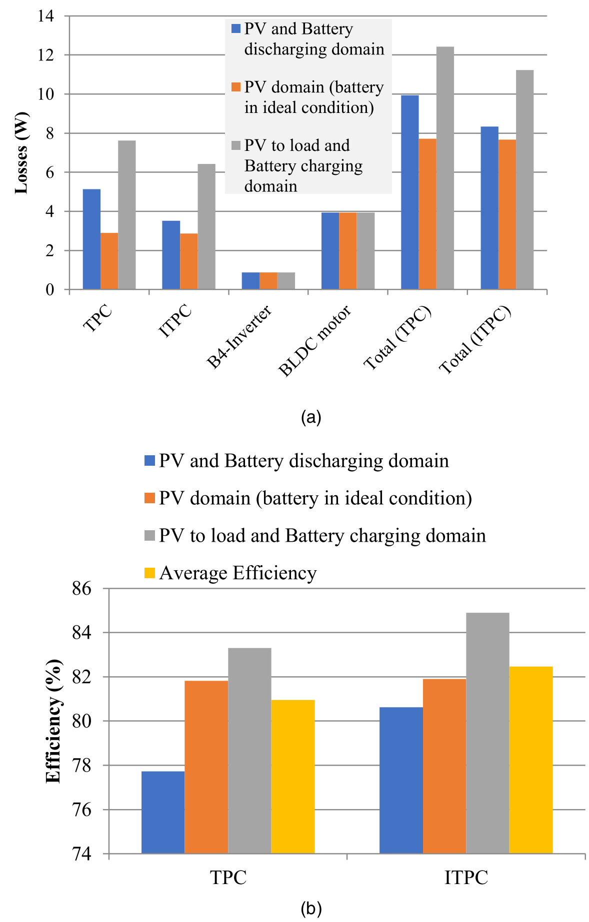

FIGURE 17. **Analysis in the proposed system under three different domains at single-stage conversion (a) Losses (b) Efficiency.**

error generator, Output Voltage Controller (OVC), Capacitor Voltage Controller (CVC) and a PWM generator The torque value 0.125 the ripple is very less.

A. LOSSES AND EFFICIENCY ANALYSIS OF CONVENTIONAL AND PROPOSED SYSTEM

The losses in the total framework cause problems in different segments, for example, converter, B4-Inverter, and the BLDC drive. The losses in these three segments are dissected for three distinct setups of the proposed research, for example, battery releasing area, PV space and battery charging space individually, as appears in Figure 16(a). From the figure, the losses in PV, battery charging, and battery releasing area are higher in TPC because of the utilization of battery-powered bidirectional converter tied at DC interface, which builds the exchanging losses and battery volume in the framework. Be that as it may, TPC, battery-controlled bidirectional converter tied at inductor terminals, in this way losses are extensively decreased. Hence, a huge increment inefficiency on the range of 1.5–2% is accomplished in the proposed arrangement as appeared in Figure 16(b). The losses in these three segments are dissected for three distinct setups of the proposed research, for example, battery releasing area, PV space, and battery charging space individually as appeared in Figure 17(a). From the figure, the losses in PV, battery charging and battery releasing area are higher in TPC because of the utilization of battery-powered bidirectional converter tied at DC interface, which builds the exchanging misfortunes and battery volume in the framework. Be that as it may, ITPC, battery-controlled bidirectional converter tied at inductor terminals, in this way losses are extensively decreased. Hence, an increment inefficiency in the range of 1.5%–2% is accomplished in the proposed arrangement as appears in Figure 17(b).

IV. EXPERIMENTAL ANALYSIS OF ITPC AND B4-INVERTER FED BLDC MOTOR DRIVER

The experimental verification is conducted for validating the proposed ITPC and B4-Inverterfed BLDC motor drive. The hardware of ITPC and B4-Inverter fed BLDC motor drive is presented in Figure 18.The hardware ITPC and B4-Inverter fed BLDC motor drive consists of 16-Bit digital signal Peripheral Interface Controller (dsPIC30F4011) for ITPC control, 32-Bit Mixed-Signal Microcontroller (MSP432P401R) for B4-Inverter control, a gate driver circuit for ITPC and B4-Inverter MOSFETs. The feedback signals are processed with the help of measurement devices

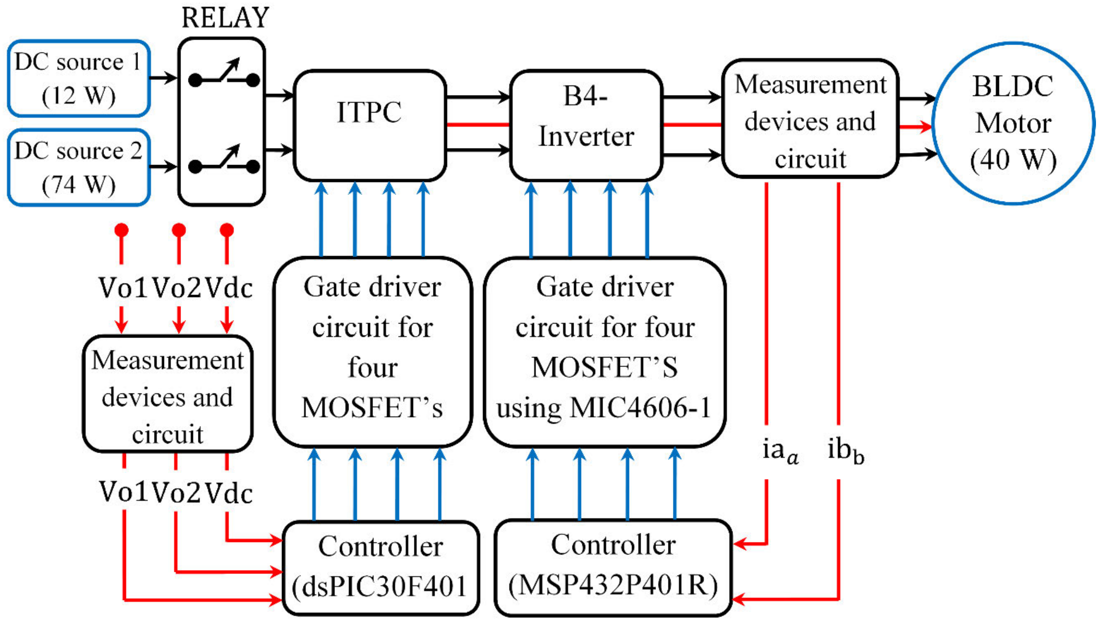

FIGURE 18. Experimental illustration for ITPC and B4-Inverterfed BLDC motor drive, consisting of 16-Bit digital signal Peripheral Interface Controller (dsPIC30F4011) for ITPC control, 32-Bit Mixed-Signal Microcontroller (MSP432P401R) for B4-Inverter control, a gate driver circuit for ITPC and B4-Inverter MOSFETs.

and circuit, and thereafter the control signals to the ITPC and B4-Inverter are transmitted by a dsPIC30F4011 and MSP432P401R.The ITPC is coupled among PV, Battery and load ports. A 40W BLDC motor is powered by a B4-Inverter in the form of a load port of the new system. The ITPC input power is changed from 12 W to 74 W which in turn, is utilized for exemplifying the performance of the proposed system.

A. CONTROLLER FEATURES OF MSP432P401R

The MSP432P401R device family is from Texas Instruments and it is the recent addition to its collection of highly efficient ultra-low-power mixed signal microcontroller units. It includes the ARM Cortex-M4 processor in an extensive configuration of device options that consists of a huge set of analog, timing, and communication peripherals, thereby providing an array of application scenarios in which both resourceful data processing and improved low-power operation are dominant. The dsPIC30F4011 controller is a popular 16-Bit controller. It also has significant features such as modified RISC CPU, CMOS technology, motor control PWM module, analog and digital signal controller features and so on.

B. MEASUREMENT DEVICES AND CIRCUIT OF ITPC

The voltage and current measurements are necessary for carrying out the control operation in microcontrollers. Hence the voltage and current transducers are needed for measuring the respective input voltage, input current, output voltages, DC link voltage, and stator currents. The voltage transducer (LV25-P) is utilized to transform the DC voltage of input

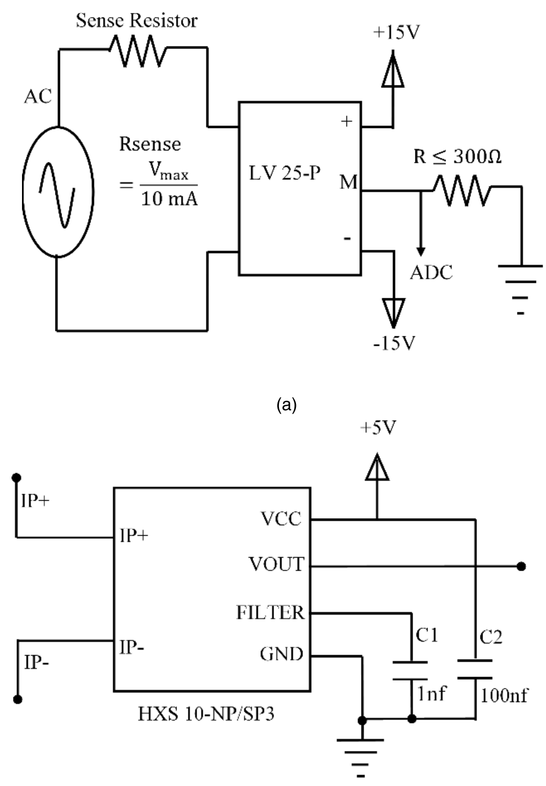

FIGURE 19. Measurement devices: (a) Voltage Transducer (LV25-P) and (b) Current transducer (HXS 10-NP/SP3).

and output within the range of 0-5V. LV25-P is a voltage sensor, though it senses current actually. A sense resistor

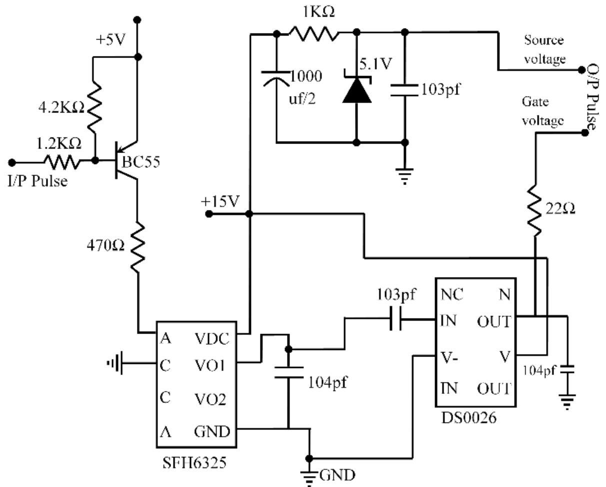

FIGURE 20. A single MOSFET driver circuit of ITPC, consisting of BC557-PNP type transistor and SFH6325, dual-channel optocoupler with a Gallium-Aluminum-Arsenide (GaAIAs) infrared emitting diode.

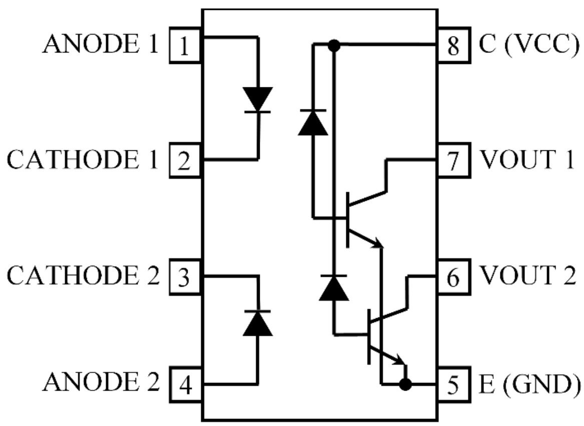

FIGURE 21. Representation of optocoupler SFH6325 equivalent circuit, showing 8 pins for 2 anodes, 2 cathodes, 1 source, and ground with 2 pins for output.

is required to reduce the current prior to its being fed into LV25-P. The output of LV25-P is current, but the analog to digital conversion (ADC) module takes only the voltage signal rather than the current signal. A resistor is kept at the output side for the purpose of converting the current to voltage. The current transducer (HXS 10-NP/SP3) works on the principle of the fundamental Hall effect measurement. Then the induced voltage at their outputs is integrated so as to get both the amplitude and phase information for the current that is being measured. The measurement devices and their equivalent circuit diagram are illustrated in Figure 19.

C. GATE DRIVER CIRCUITS FOR MOSFETS

The gate driver circuit is a typical power amplifier that gets a low-power input from a controller and generates the suitable high-current gate drive for a power MOSFET. A single MOSFET driver circuit of ITPC, is illustrated in Figure 20.

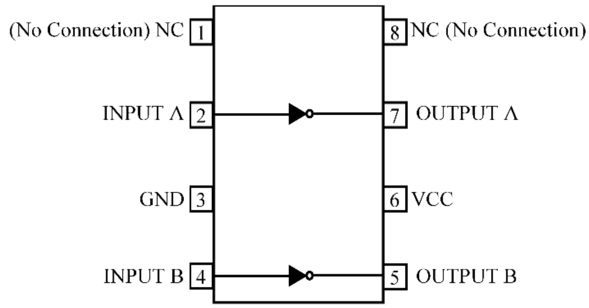

FIGURE 22. Driver IC DS0026 equivalent circuit, showing 2 input, 2 output, 2 no connection pins with 2 pins for voltage supply.

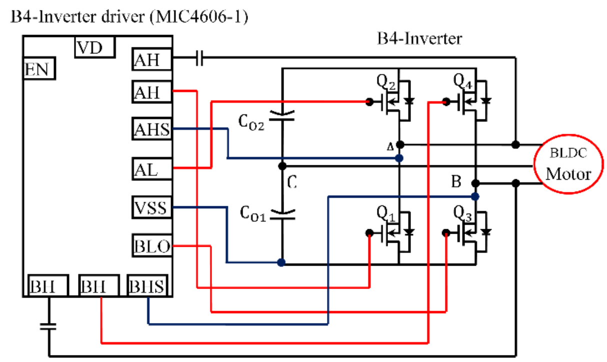

FIGURE 23. B4-Inverter MOSFET driver MIC4606-1 equivalent circuit, interfaced with the BLDC motor connected with the AH, AL, BLO, and BH pins of the driver to the gate of the B4-inverter.

Necessarily in driver circuit, BC557-PNP type transistor is employed for amplifying the current at emitter and collector terminals. The amplified current from the transistor is fed into the optocoupler (SFH6325) for providing isolation between controller and MOSFET. The SFH6325 is a dual-channel optocoupler with a Gallium-Aluminum-Arsenide (GaAIAs) infrared emitting diode, which is optically coupled with an integrated photodetector consisting of a photodiode along with a high-speed transistor in a DIP-8 plastic package. Signals can be carried between two electrically isolated circuits till the frequency of 2 MHz. The strong difference between the circuits that have to be coupled must not go beyond the maximum acceptable reference voltages. The SFH6325 equivalent circuit diagram is provided in Figure 21.

In the gate driver circuit, to transform the Transistor-Transistor Logic (TTL) level signals into high current outputs and voltages until 15V, the driver integrated circuit (driver IC) DS0026 is necessary. DS0026 is an economic monolithic high speed, two-phase Metal-Oxide-Semiconductor (MOS) clock driver and interface circuit. An exclusive circuit design outputs very high-speed operation and the capability of driving big capacitive loads. The device takes in standard TTL outputs and then has them converted to MOS logic levels. The device may be powered from standard 54/74 series and 54S/74S series gates and flip-flops. The DS0026 is supposed for use in applications where the output pulse width is controlled logically i.e., and the output pulse width is equivalent

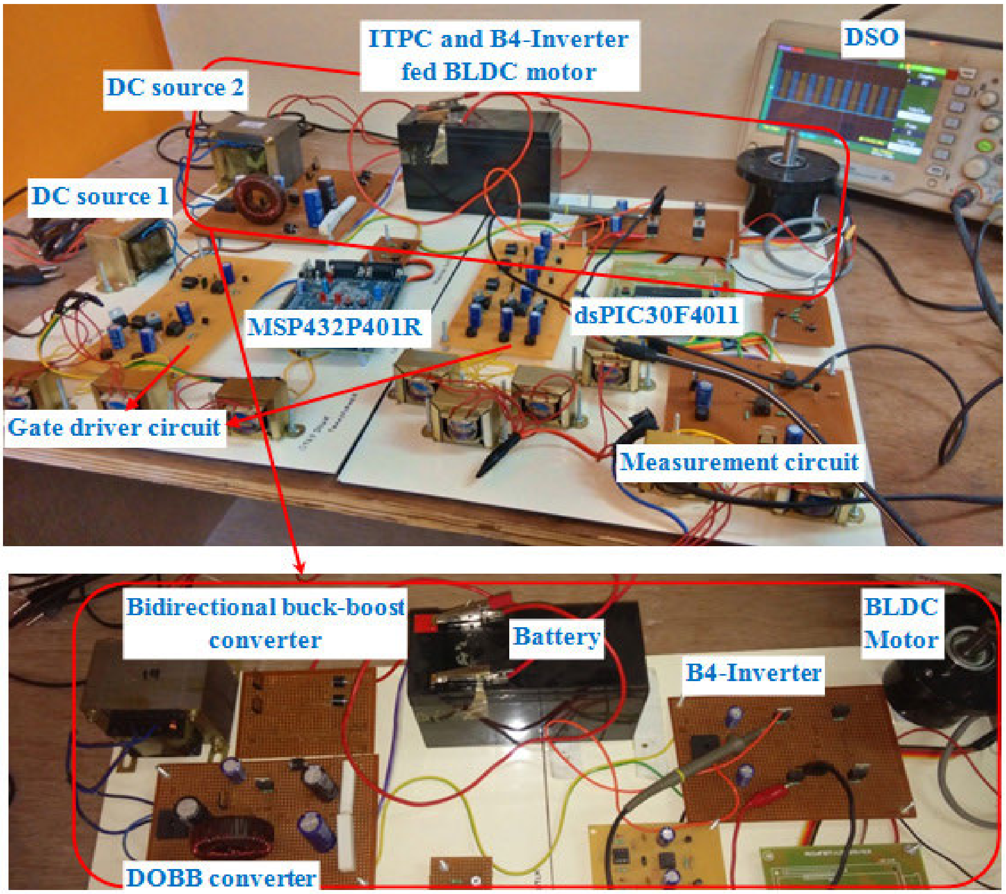

FIGURE 24. Snapshot of the test setup of proposed ITPC, showing 2 DC sources with the driver circuit, measurement circuit, and 2 controllers. The ITPC and B4-inverter fed BLDC motor is enlarged to show the converter, inverter and motor with the energy storage.

to the input pulse width. The DS0026 is developed in order to satisfy various MOS interface requirements, as illustrated in Figure 22.

In contrast, the MIC4606-1 is a B4-Inverter MOSFET driver, which characterizes an adaptive dead time and shoot-through protection, as indicated in Figure 23. The adaptive dead time circuitry monitors both the sides of the B4-Inverter actively, so as to reduce the time between high-side and low-side MOSFET transitions, thereby increasing the power efficiency. Anti-shoot through circuitry helps in preventing erroneous inputs and noise from turning both MOSFETs of every side of the bridge ON simultaneously. The MIC4606- also renders a wide 5.5 V to 16 V operating supply range for maximizing the system efficiency. The low 5.5 V operating voltage permits for long-duration run times in battery-powered applications. Moreover, the MIC4606-1's adjustable gate drive fixes the gate drive voltage for optimal MOSFET drain-source resistance that reduces the power loss.

D. HARDWARE COMPONENT SELECTION

A 40 W, 48 V, 0.83 Amp BLDC Motor load is chosen for the purpose of test studies. Hence, the ITPC and B4-Inverter are developed for coupling PV, battery, and BLDC motor. The voltage control is got by changing the duty cycle (D), which is decided by Equation (12) [6]

$$D = \frac{V_{dc}}{V_{in} + V_{dc}} = 48/(16.6 + 48) = 0.74 \quad (12)$$

where (V_{in}) represents input DC voltage at normal condition, while (V_{dc}) indicates the DClink voltage, i.e., input voltage of B4-Inverter.The inductor (L_1) value is obtained by Equation (13) below [6]

$$L_1 = \frac{(V_{dc})^2}{P_{dc}} \times \frac{(1-D)^2}{2 \times f_{SW}} = \frac{(48V)^2}{40W} \times \frac{(1-0.74)^2}{2 \times 10000} = 194.68\mu H \quad (13)$$

where, f_{SW} is the switching frequency and P_{dc} is the DC link power (input and output power of B4 inverter)

The input inductance values are taken at lesser than1/10th of the minimum critical value of inductance so as to guarantee a deep DCM condition [7]. Therefore, the value of inductor (L_1) is chosen around1/10th of the critical inductance and is taken at 19.5μH.Here, (f_{SW}) refers to the switching frequency, (P_{dc}) indicates the DC link power (i.e., the input power of B4-Inverter).The rating of the output capacitors

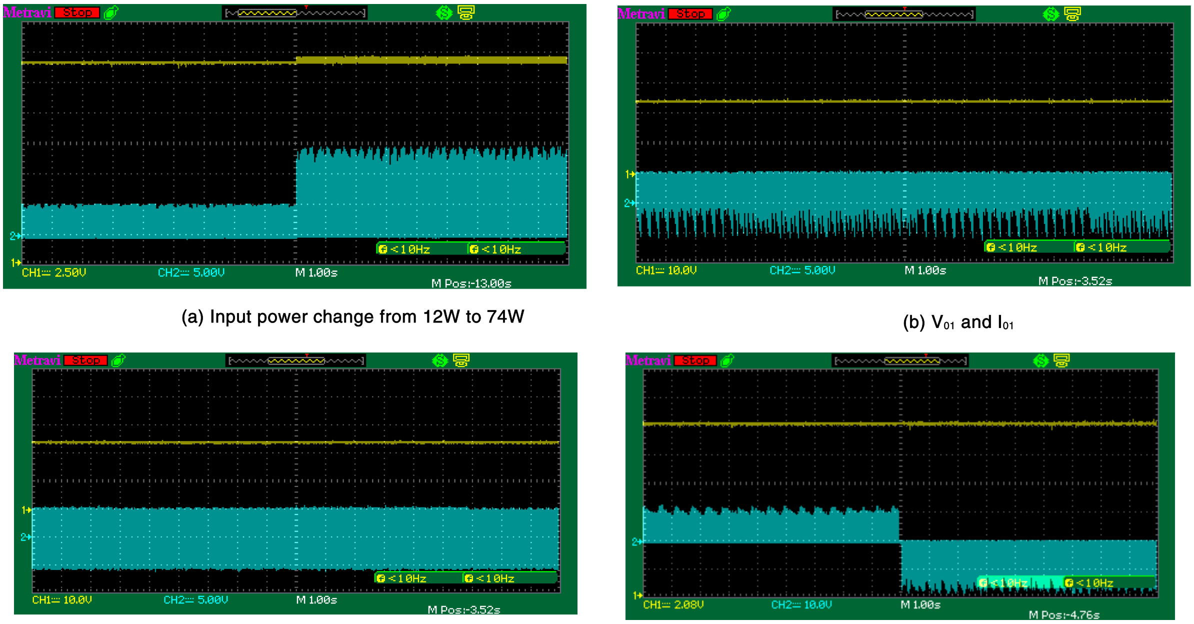

(a) Input power change from 12W to 74W

(b) V_{01} and I_{01}

(c) V_{02} and I_{02}

(d) V_{bat} and I_{bat}

FIGURE 25. Prototype input/output parameter responses due to varied output power for the BLDC treated as a load port.

$C_{01} and\ C_{02}$ is derived from Equation (14) below for the minimum pulse width as done by [4]

$$C_{01,02} = \frac{I_{dc}}{\sim V_{dc} \times \omega_f \times 2} = \frac{0.83}{(0.03 \times 48) \times 314 \times 2} = 917\mu F \quad (14)$$

where (ω_f) indicates the angular frequency, permissible ripple voltage $(\sim V_{dc})$ in the output capacitors $(C_{01} and\ C_{02})$, which is considered to be the closest possible value, and therefore the output capacitors value of $1000\mu F$ is chosen.

The current rating of ITPC converter and B4-Inverter switches is estimated by Equation (15,16) [9]

$$I_{SWITCH} = safetymargin I_{dc} + \approx I_{DC} \quad (15)$$

$$I_{SWITCH} = 1.25\,\{0.83 + 0.8715\} = 1.0893A \quad (16)$$

where I_{dc} represents the DC link current (i.e., the input current of B4-Inverter), $\approx I_{DC}$ is the output ripple current in the ITPC converter and B4-Inverter, which is taken as 5% of maximum current and is computed as 0.08715 A, and the safety margin is taken to be 1.25 for the purpose of design. Likewise, the voltage rating of the ITPC converter and B4-Inverterswitches is estimated by means of Equation (17,18)

$$V_{SWITCH} = safetymargin \times V_{dc} \quad (17)$$

$$V_{SWITCH} = 1.25 \times 48V = 60V \quad (18)$$

From the earlier equations, the maximum voltage across the device can be 60 V, and the current passing through the device could be 1.09 A. The ITPC and B4-Inverter fed BLDC motor driver constructed with the key parameters that are presented in Table 2.

TABLE 2. ITPC and B4-Inverter fed BLDC motor driver components specification.

Sl.no.	Components	Specification
1	N-Channel Power MOSFETs $(S_1, S_2, S_3\ and\ S_4)$ and $(Q_1, Q_2, Q_3\ and\ Q_4)$	100 V, 30 A
	Part Number: IRF540	
2	Input inductor (L_1) Core type: "Round" Size: T45*26*15 ring Toroidal ferrite core Copper gauge: "25"	19.5 μH
3	Power diodes $(D_1, D_2, D_3\ and\ D_4)$ Part number: 6A04	400 V, 6A
4	Intermediate capacitor (C_1)	5 mH
5	Output capacitors $(C_{o1}\ and\ C_{o2})$	1000 μF, 100 V
6	Load: BLDC Motor Model number: UEL055-S100055-D1	40 W, 48 V, 0.83 A
7	Controller1: dsPIC30F4011 Controller2: MSP432P401R	16-Bit 32-Bit

E. EXPERIMENTAL RESULTS OF THE PROPOSED ITPC

For verifying the efficiency of the system proposed, a low power range laboratory prototype is constructed as illustrated in Figure 24. For the experimental arrangement, two diverse input power sources are used. A power supply with the electric specification of 16.6 V, 0.72 A, 12 W, and 16.9 V, 4.38 A, 74 W are considered to be the input power sources. Moreover, a lead-acid battery having the electric specification of 12 V and 7.4 Ah gets implemented, considering the output load

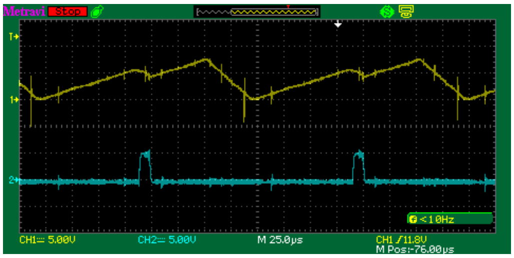

(a) $i_{L1} and i_{S2}$ at 12 W condition

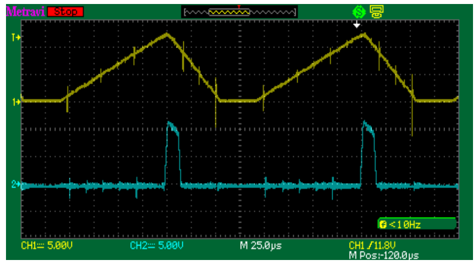

(b) $i_{L1} and i_{S2}$ at 74 W condition

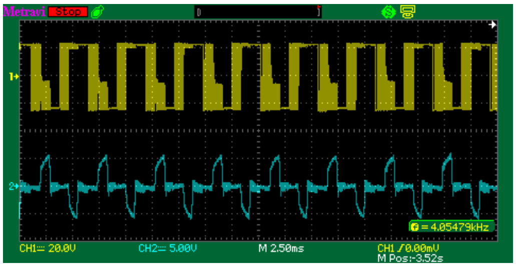

(c) $e_{a} and i_{a}$ at 12 and 74 W condition

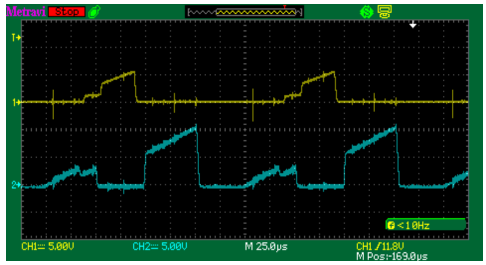

(d) $v_{bat} and i_{bat}$ at 12 W condition

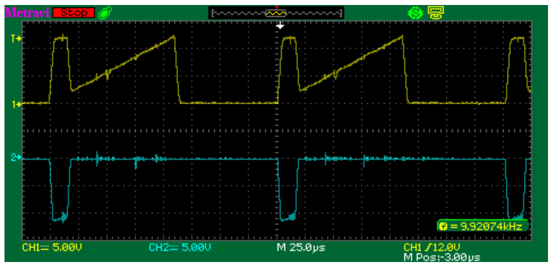

(e) $v_{bat} and i_{bat}$ at 74 W condition

FIGURE 26. Detailed waveforms of the proposed system with the output power variation from 12 W to 75 W with respect to ITPC parameters, BLDC motor parameters and battery parameters.

TABLE 3. Experimental specification of the proposed system.

Sl. No	Objects	Values
1	DC power source 1	16.6 V, 0.72 A and 12 W
2	DC power source 2	16.9 V, 4.38 A, and 74 W
3	Battery power source	12 V, 7.4 Ah, and 88.8 Wh
4	ITPC output voltage	48 V
5	ITPC output current	0.83 A
6	ITPC output power	40 W
7	Rated BLDC motor power (Torque = 0.125 Nm, Speed = 2800 rpm, DC link voltage = 24V, number of poles = 8)	39 W

in the auxiliary circuit, backup power supply. The prototype parameters of the proposed system are given in Table 3.

For the experimental analysis, the DC power supply is fixed at a constant voltage value of 16.7 V, but diverse current ratings that can indicate PV source effects on insolation variation conditions are set. The control scheme is realized by dsPIC30F4011 and MSP432P401R. The parameters like ITPC output voltages ($V_{01} and\ V_{02}$), ITPC output currents ($I_{01} and\ I_{02}$), stator voltage (e_a), stator current (i_a), battery voltage $v_{bat}()$ and battery current (i_{bat}) of the system are measured for the validation of the proposed technique.The prototype preparation is analyzed in two diverse operation modes i.e. battery charging and battery discharging, of ITPC. At the start, input source 1(12 W) is used on ITPC fed BLDC motor driver system. Later, the input power applied is increased abruptly from 12 W to 74 W, as indicated in Figure 25(a).The BLDC motor of power rating 39W is treated to be the load port of the proposed system. Therefore, the ITPC must provide 40 W of electrical power to a B4-Inverter fed BLDC motor. The motor supplies 40 W of mechanical power to a load at 2800 rpm. From Figure 25(b) and (c), the output voltages of the ITPC can be controlled with stability to be ($V_{01} and V_{02} = 24\ V$) and the average output currents ($I_{01} and I_{02} = 0.83\ A$) under the total output power variation between 12 and 74 W. At low power, i.e., 12W condition, the necessary load power of 32.15W is extracted with efficiency from the battery. At a certain period of time, 11.9 V and +2.701 A is obtained from the battery. In a similar manner, at maximum power (i.e.74 W) condition, the extra

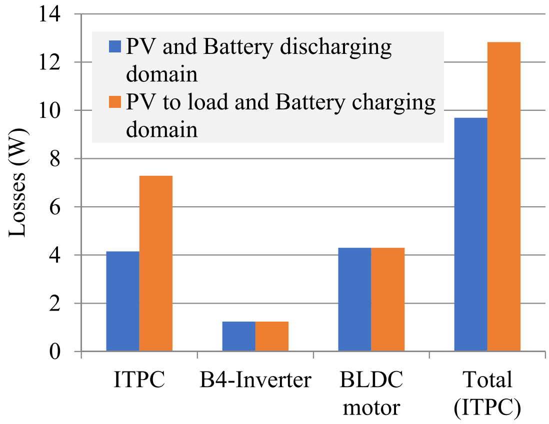

(a)

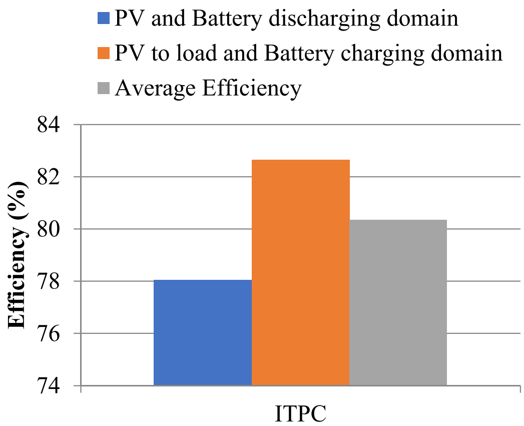

(b)

FIGURE 27. Test analyses in the proposed system under two different domains (a) Losses, (b) Efficiency for different parameters pertaining to PV, battery, and load.

power of 26.71 W is deposited efficiently to the battery. At a specific instance, 12.8 V and -2.087 A is applied towards the battery as illustrated in Figure 25(d). As observed from the figure, the battery current waveform is maintained above zero points, and then transferred to below zero points, indicating that the battery supplies/get the energybased on the PI closed-loop voltage control.

Furthermore, the elaborate waveforms of the system proposed through the ITPC parameters ($i_{L1}, i_{S2}, I_{01}, I_{02}$), BLDC motor parameters (e_a, i_a) and Battery parameters (V_{bat}, I_{bat}) with the output power variation from 12 W to 75 W is demonstrated in Figures 26 (a)-(e).

The losses in these three domains, i.e. converter, B4-inverter and BLDC motor, are evaluated for two diverse configurations of battery charging and battery discharging through the experimental arrangement, as illustrated in Figure 27. From the test analysis, it is verified that the losses of the proposed ITPC get reduced and the efficiency of the converter improved.

V. CONCLUSION

The Three Port Converter (TPC) and B4-Inverter fed BLDC motor drive has been proposed targeting low or medium power applications. The TPC has been operated in unidirectional and bidirectional ways simultaneously for achieving an inherent dual voltage and power flow control. Furthermore, losses and efficiency of the proposed system are analyzed with three different domains, i.e., with battery charging, discharging, and PV systems effectively. The results have been validated by performing simulations of the proposed systems in MATLAB/Simulink. A detailed comparison has been made between the proposed converter and the predecessors to examine the benefits of the proposed converter. Experimentation has been performed using prototype models, the hardware results of which have closely resembled the simulation results. Moreover, a satisfactory closed-loop performance has been achieved for both simulation and experimental setup. Losses and efficiency of the proposed ITPC based system are compared with the existing TPC based system. The validation results reveal that the proposed converter has performed effectively under all the three domains and that the losses in the PV domain has been reduced compared to the other converters. In addition, the average efficiency achieved has been 80.95%. The outcomes of the experiment have validated the proposed model for different applications related to renewable sources and energy storage systems. Future work of the research will focus on the application of the proposed converter in the domain of agriculture, integrating renewables and energy storages.

REFERENCES

[1] M. A. S. Masoum, S. M. M. Badejani, and E. F. Fuchs, "Microprocessor-controlled new class of optimal battery chargers for photovoltaic applications," *IEEE Trans. Energy Convers.*, vol. 19, no. 3, pp. 599–606, Sep. 2004.
[2] H. Zhu, D. Zhang, B. Zhang, and Z. Zhou, "A nonisolated three-port DC-DC converter and three-domain control method for PV-battery power systems," *IEEE Trans. Ind. Electron.*, vol. 62, no. 8, pp. 4937–4947, Aug. 2015.
[3] Y.-M. Chen, A. Q. Huang, and X. Yu, "A high step-up three-port DC–DC converter for stand-alone PV/battery power systems," *IEEE Trans. Power Electron.*, vol. 28, no. 11, pp. 5049–5062, Nov. 2013.
[4] T. Arthi and V. Sivachidambaranathan, "Fuzzy controlled three port DC-DC converter fed DC drive for PV system," in *Proc. Int. Conf. Comput. Power, Energy Inf. Commun. (ICCPEIC)*, Chennai, India, Apr. 2016, pp. 425–429.
[5] P. M. Kishore and R. Bhimasingu, "Improving the performance of hybrid microgrid using isolated three-port converter," in *Proc. IEEE 1st Int. Conf. Power Electron., Intell. Control Energy Syst. (ICPEICES)*, New Delhi, India, Jul. 2016, pp. 1–6.
[6] A. Emadi, A. Khaligh, Z. Nie, and Y. J. Lee, *Integrated Power Electronic Converters and Digital Control*. Boca Raton, FL, USA: CRC Press, 2009.
[7] D. S. L. Simonetti, J. Sebastian, F. S. dos Reis, and J. Uceda, "Design criteria for SEPIC and Cuk converters as power factor preregulators in discontinuous conduction mode," in *Proc. Int. Electron. Motion Control Conf.*, vol. 1, 1992, pp. 283–288.
[8] S. Shuvo, E. Hossain, T. Islam, A. Akib, S. Padmanaban, and M. Z. R. Khan, "Design and hardware implementation considerations of modified multilevel cascaded H-bridge inverter for photovoltaic system," *IEEE Access*, vol. 7, pp. 16504–16524, 2019.
[9] B. Singh, S. Singh, A. Chandra, and K. Al-Haddad, "Comprehensive study of single-phase AC-DC power factor corrected converters with high-frequency isolation," *IEEE Trans. Ind. Informat.*, vol. 7, no. 4, pp. 540–556, Nov. 2011.
[10] S. K. Shanmugam and A. Senthilkumar, "Design and implementation of DC source fed improved dual-output buck-boost converter for agricultural and industrial applications," *J. Vibroengineering*, vol. 19, no. 8, pp. 6433–6454, Dec. 2017.

[11] S. K. Shanmugam, S. Arumugam, G. Palanirajan, M. Ramachandran, and K. K. Kanagaraj, "Implementation of solar photovoltaic array and battery powered enhanced DC-DC converter using B4-inverter fed brushless DC motor drive system for agricultural water pumping applications," *J. Vibromotorering*, vol. 20, no. 2, pp. 1214–1233, 2018.

[12] S. K. Shanmugam, M. Ramachandran, K. K. Kanagaraj, and A. Loganathan, "Sensorless control of four-switch inverter for brushless DC motor drive and its simulation," *Circuits Syst.*, vol. 7, no. 6, pp. 726–734, 2016, doi: 10.4236/cs.2016.76062.

[13] S. Sathishkumar, R. Meenakumari, E. Jobanarubi, P. J. S. Anitta, and P. RavikuMar, "Microcontroller based BLDC motor drive for commercial applications," in *Power Electronics and Renewable Energy Systems* (Lecture Notes in Computer Science), vol. 326, C. Kamalakannan, L. Suresh, S. Dash, and B. Panigrahi, Eds. New Delhi, India: Springer, 2015, pp. 829–841.

[14] S. K. Shanmugam, K. Muthusamy, V. Sennippan, S. Balasubramaniam, and S. Ramasamy, "Modelling of solar photovoltaic array fed brushless DC motor drive using enhanced DC-DC converter," *Proc. Romanian Acad. A, Math., Tech. Sci., Inf. Sci.*, vol. 20, no. 2, pp. 164–173, Jun. 2019.

[15] J. Deng, H. Wang, and M. Shang, "An integrated three-port DC/DC converter for high-voltage bus based photovoltaic systems," in *Proc. IEEE Energy Convers. Congr. Expo. (ECCE)*, Sep. 2018, pp. 5948–5953.

[16] J. Jasper and G. Chandran, "A comparative investigation on DTC of B4-inverter-fed BLDC motor drives using PI and intelligent controllers," *Int. J. Adv. Res. Elect., Electron. Instrum. Eng.*, vol. 4, no. 3, 2015.

[17] M. Heydari, M. Mohamadian, A. Fatemi, and A. Y. Varjani, "Three-phase dual-output six-switch inverter," *IET Power Electron.*, vol. 5, no. 9, pp. 1634–1650, Nov. 2012.

[18] S. K. Shanmugam, S. Subramaniam, K. K. Kanagaraj, A. Loganathan, and A. Subramanian, "Modeling and simulation of renewable energy fed brushless DC motor drive using improved DC-DC converter for reducing vibration and noise," *J. Elect. Electron. Syst.*, vol. 7, no. 274, pp. 2332–2796, 2018.

[19] R. M. Pindoriya, A. K. Mishra, B. S. Rajpurohit, and R. Kumar, "FPGA based digital control technique for BLDC motor drive," in *Proc. IEEE Power Energy Soc. Gen. Meeting (PESGM)*, Portland, OR, USA, Aug. 2018, pp. 1–5.

[20] J. Babu and R. Radhika, "FPGA based implementation of brushless DC motor drive using single current sensor and comparison with conventional method," in *Proc. IEEE Int. Conf. Power, Control, Signals Instrum. Eng. (ICPCSI)*, Sep. 2017, pp. 703–709.

[21] X. Zhou, X. Chen, C. Peng, and Y. Zhou, "High performance nonsalient sensorless BLDC motor control strategy from standstill to high speed," *IEEE Trans. Ind. Informat.*, vol. 14, no. 10, pp. 4365–4375, Oct. 2018.

[22] S. Geraee, M. Shafiei, A. R. Sahami, and S. Alavi, "Position sensorless and adaptive speed design for controlling brushless DC motor drives," in *Proc. North Amer. Power Symp. (NAPS)*, Sep. 2017, pp. 1–6.

[23] F. Z. Peng, "Z-source inverter," *IEEE Trans. Ind. Appl.*, vol. 39, no. 2, pp. 504–510, Mar./Apr. 2003.

[24] F. D. Kieferndorf, M. Forster, and T. A. Lipo, "Reduction of DC bus capacitor ripple current with PAM/PWM converter," *IEEE Trans. Ind. Appl.*, vol. 40, no. 2, pp. 607–615, Mar./Apr. 2004.

SATHISH KUMAR SHANMUGAM received the Ph.D. degree from the Faculty of Information and Communication Engineering, Anna University, Chennai, India, in 2017. He currently works as an Associate Professor with the Department of EEE, M. Kumarasamy College of Engineering, Karur, India. He has 15 years of teaching experience. His current research interests include control, embedded systems, modeling, and power electronic converter. In addition, he is a Reviewer of the IEEE TRANSACTIONS OF INDUSTRIAL ELECTRONICS, IEEE ACCESS, *ETRI Journal*, the *Journal of Electrical Engineering Technology*, *JVE*, *JME*, and *MME*.

SASIKALA RAMACHANDRAN received the master's degree in engineering from the Thanthai Periyar Government Institute of Technology, Bagayam, Vellore. She is currently working as an Assistant Professor with the Department of Electronics and Communication Engineering, Kongu Engineering College. Her research interests include smart grid monitoring, communications, power quality, and data analytics and its visualization. She holds professional body membership like IAENG and ASDF Societies. She is actively associated with the IEEE societies, Smart Grid, and the Power Electronics Society. She currently serves as the IEEE Webex-Smart Grid R and D Committee Member. She had 13 years of experience in the field of teaching. She has published 22 articles in International Journals, Conferences, and National Conferences out of which two are Scopus indexed Journals and an SCI indexed journals. Since March 2009, she has been with the Kongu Engineering College. She has been accepted as a Reviewer/Speaker from ASDF. She is an active Publon ID Holder. She is an Active Member in Smart Energy Consumer Collaborative (SECC) Society.

SENTHILKUMAR ARUMUGAM received the B.E. degree in electrical and electronics engineering from the Kumaraguru College of Technology, Bharathiar University, India, in 1995, and the M.E. degree in power Electronics and Drives from the Sri Ramakrishna Engineering College, Anna University, Chennai, in 2006. He currently works as a Senior Assistant Professor with the Chettinad College of Engineering and Technology, affiliated to Anna University, Chennai, where he is also a Research Scholar.

SANJEEVI PANDIYAN received the M.S. degree in software engineering and Ph.D. degree from VIT, Vellore, India. He is currently a Postdoctoral Fellow with the Key Laboratory of Advanced Process Control for Light Industry, Jiangnan University, China, Ministry of Education. He worked as an Assistant Professor with VIT Bhopal University, from 2018 to 2019. He has been associated with the Ramco Systems in Research and Development Team, for one year. He has published several conference and journal articles. He is active in the research areas of computer science and remote sensing, where he has published extensively. His current research interests include software systems, the Internet of Things (IoT), job scheduling in distributed environments, distributed algorithms, drought detection in remote sensing, and cloud computing. He also serves as a Reviewer of the IEEE SENSORS JOURNAL, *ACM Transactions on Internet Technology*, the *European Journal of Remote Sensing, Computers, and Electrical Engineering*, *ACM Transactions on Asian and Low-Resource Language Information Processing*, *IET Intelligent Transport Systems*, *Transactions on Emerging Telecommunications Technologies*, and the *Journal of Supercomputing*.

ANAND NAYYAR (Senior Member, IEEE) received the Ph.D. degree in computer science from Desh Bhagat University, in 2017, in the area of wireless sensor networks. He is currently working with the Graduate School, Duy Tan University, Da Nang, Vietnam. He is a Certified Professional with more than 75 Professional certificates from CISCO, Microsoft, Oracle, Google, Beingcert, EXIN, GAQM, Cyberoam, and many more. He has published more than 300 research papers in various National and International Conferences, and International Journals (Scopus/SCI/SCIE/SSCI Indexed). He is a member of more than 50 associations, as a Senior Member and a Life Member, and also acting as ACM Distinguished Speaker. He has authored/coauthored cum Edited 30 Books of Computer Science. He associated with more than 400 International Conferences as Program Committee/Advisory Board/Review Board Member. He has two Patents to his name in the area of the Internet of Things, speech processing. He is currently working in the area of wireless sensor networks, manets, swarm intelligence, cloud computing, the Internet of Things, blockchain, machine learning, deep learning, cyber security, network simulation, and wireless communications. He was a recipient of more the 25 Awards for the Teaching and Research–Young Scientist, the Best Scientist, the Young Researcher Award, the Outstanding Researcher Award, the Indo-International Emerging Star Award (to name a few). He is acting as Editor-in-Chief for *IGI-Global Journal* and the *International Journal of Smart Vehicles and Smart Transportation*.

EKLAS HOSSAIN (Senior Member, IEEE) received the B.S. degree in electrical and electronic engineering from the Khulna University of Engineering and Technology, Bangladesh, in 2006, the M.S. degree in mechatronics and robotics engineering from the International Islamic University of Malaysia, Malaysia, in 2010, and the Ph.D. degree from the College of Engineering and Applied Science, University of Wisconsin Milwaukee (UWM). He has been working in the area of distributed power systems and renewable energy integration for last ten years and he has published a number of research articles and posters in this field. He is involved with several research projects on renewable energy and grid tied microgrid system at Oregon Tech, as an Associate Professor with the Department of Electrical Engineering and Renewable Energy. He is a Senior Member of the Association of Energy Engineers (AEE). He is currently serving as an Associate Editor of IEEE Access. He is working as an Associate Researcher with the Oregon Renewable Energy Center (OREC). He is a registered Professional Engineer (PE) in the state of Oregon, USA. He is also a Certified Energy Manager (CEM) and a Renewable Energy Professional (REP). His research interests include modeling, analysis, design, and control of power electronic devices, energy storage systems, renewable energy sources, integration of distributed generation systems, microgrid and smart grid applications, robotics, and advanced control system. He is the winner of the Rising Faculty Scholar Award from the Oregon Institute of Technology for his outstanding contribution in teaching, in 2019. He is with his dedicated research team, is looking forward to explore methods to make the electric power systems more sustainable, cost-effective and secure through extensive research and analysis on energy storage, microgrid systems, and renewable energy sources.